Cometary impacts an unlikely pathway towards the origins of life on Earth

Richard J. Anslow[1*], Catriona H. McDonald[1], Amy Bonsor[1], Paul B. Rimmer[2], Auriol S. P. Rae[3]

[1]Institute of Astronomy, University of Cambridge, Madingley Road, Cambridge, CB3 0HA, UK.

[2]Cavendish Laboratory, University of Cambridge, JJ Thomson Ave, Cambridge, CB3 0HE, UK.

[3]School of Geosciences/Edinburgh Centre for Planetary Sciences,

University of Edinburgh, Edinburgh, EH9 3FE, UK.

[*]Corresponding author. Email: rja92@cam.ac.uk

An early period of cometary bombardment has long been speculated to provide an important source of prebiotic feedstock molecules, required for the origins of life on Earth. In support of this interpretation, comets boast a rich diversity of volatile organic molecules, with many thought to be limiting for prebiotic chemistry. Modelling studies suggest, however, that a significant proportion of these molecules will be destroyed during hypervelocity impact. Here, we revisit the ability of comets to deliver prebiotic feedstock molecules, leveraging recent advances in cometary impact simulations, comet-atmosphere interactions, and dynamical modelling of short-period comets' origin and evolution. Taken together, the rapid decline in Earth's cometary impact bombardment and the efficient destruction of fragile cometary organics indicate that the successful delivery of prebiotic feedstock molecules was an exceedingly rare event. Our results therefore challenge the long-held assumption that cometary impacts played an important role in the origins of life on Earth.

Introduction

The origin of life on Earth presumably resulted from prebiotic chemistry, the synthesis of key molecular building blocks from an initial reservoir of reactive bioessential feedstock molecules (*1*). Hydrogen cyanide (HCN) has emerged as a key feedstock molecule, with its high-energy triple (nitrile) bond able to thermodynamically drive subsequent chemistry, and assumes a central role in several prebiotic syntheses (*2–4*). Recent experimental studies demonstrate that high concentrations ($\sim$ 10 mM) of HCN can synthesise many of the building blocks of life, including lipids, sugars, nucleobases, and nucleotides (*2–6*). Yet, the source of such a concentrated reservoir of feedstock molecules, such as HCN, on the early Earth is still debated.

Sources of HCN (and other C, H, N, and O molecules) have been historically divided into two categories: endogenous synthesis in the early terrestrial atmosphere, and exogenous delivery in the form of comets, asteroids, and interplanetary dust particles (IDPs) (*7*). The former, endogenous synthesis, is particularly sensitive to the geological context of prebiotic chemistry, with the yield of HCN production substantially higher in more reducing atmospheres (*8, 9*). There is, however, substantial geological evidence against a reducing early atmosphere (*10, 11*), and even in the transiently reducing atmospheres afforded by the late accretion of large iron-rich planetesimals, rain-out yields steady-state HCN concentrations orders of magnitude lower than used in prebiotic experiment (*12, 13*). Such planet-scale events will deliver photochemically synthesised HCN to all exposed land on the early Earth, yet will require the subsequent stockpiling and concentration of cyanide (perhaps as ferrocyanide complexes) for subsequent utility in prebiotic chemistry (*1*).

In contrast, an exogenous source of Earth's prebiotic inventory – a suggestion now more than a century old (*14, 15*) – naturally bypasses any dependence on atmospheric oxidation state, and has the potential to deliver feedstock molecules in high concentration to local environments. Chyba & Sagan (*7*) demonstrated, using analytical fits to the lunar cratering record, that the exogenous delivery of carbon would be dominated by IDPs, with the cometary delivery of organic carbon insignificant on a global scale. The carbon and nitrogen content of IDPs is, however, dominated by insoluble complex aromatic hydrocarbons (*16*), rendering IDPs a highly unlikely source of the reactive organic precursors (such as HCN) required for synthetic prebiotic chemistry. The same is not true for comets, which exhibit a rich diversity of volatile organic molecules, including most

significantly HCN at the ~ 0.1 % level relative to water (*17*). Comets therefore have the potential to deliver as much as ~ 30 mM HCN to local environments, a concentration of immediate relevance for prebiotic chemistry, and have accordingly been the subject of significant attention in origins of life research (*18–23*).

Two key lines of evidence suggest that, despite not appearing in all prebiotic chemical networks, the intact delivery of HCN represents an end-member case for the cometary delivery of prebiotic feedstock molecules. First, HCN is the only feedstock molecule observed in Solar System comets in prebiotically relevant concentrations (*17*); other key feedstock molecules such as cyanoacetylene (HC_3N) and cyanogen (NCCN) are found to be orders of magnitude less abundant (*17, 24*). Second, the triple (nitrile) bond in HCN is expected to confer much greater durability to impact pyrolysis in comparison to other (more complex) prebiotic feedstock molecules (*22*). If it conspires that comets were unable to deliver a prebiotically relevant concentration of HCN, we expect the same to be true for other prebiotic feedstock molecules.

To assess the relative importance of cometary impacts as a source of concentrated feedstock molecules, it is therefore crucial to accurately determine the ability of comets to deliver their HCN intact to the surface of the early Earth. Therein lies the crux of long-standing objections to cometary delivery, which relate to both the destruction of comets during atmospheric passage (*7, 19*), and the thermal destruction of fragile organic species during hypervelocity impact (*20, 21*). Recent modelling efforts demonstrate that only comets larger than ~ 100 m will survive passage through the early Earth's atmosphere (*25*), and that the survival of HCN during hypervelocity impact has been historically overestimated (*22*). It is thus prudent to quantitively re-examine the cometary delivery of prebiotic feedstock molecules, given that multiple lines of evidence suggest its efficacy may have been historically overestimated.

The present study uses the results of N-body simulation of short-period comet formation and evolution (*26, 27*) to reassess the potential role of cometary delivery in the origins of life on Earth. We leverage recent methodological advances in the modelling of cometary atmospheric entry (*25*) and the destruction of HCN during hypervelocity impact (*22*) to quantify the number of comets able to deliver key bioessential feedstock molecules in prebiotically relevant concentration. We find that constraints on comet size, velocity, and angle – necessary for the intact survival of comets and their HCN during hypervelocity impact – preclude a robust cometary source of concentrated

prebiotic feedstock molecules. Thus, despite the rich diversity in volatile organic species observed in Solar System comets, our results challenge the hypothesis that comets played an important role in the origins of life on Earth.

Results

Earth's early cometary bombardment

Here, we use Earth's cometary bombardment chronology (*26*) as derived from the Nesvorný et al. (*27*) model of short-period comet formation and evolution. This model, following the long-term evolution of one million primordial cometesimals originating in a disk exterior to Neptune, is calibrated against several key observational constraints from the outer Solar System (*26–28*). This approach diverges from previous modelling efforts, which instead use the lunar crater record as an indirect proxy for Earth's early cometary bombardment [e.g., (*7, 19, 20*)]. This represents an important methodological distinction, given that it is now clear that the lunar crater record neither unambiguously constrains impactor composition (*29*), nor provides a reliable record of the Moon's bombardment history pre-3.9 Gya (*30*). Indeed, since the lunar crater record is consistent with an asteroidal origin (*31*), it appears unlikely that it will accurately constrain Earth's early cometary bombardment.

To reproduce the observed distribution of modern short-period comets, such dynamical models require some mechanism to limit the physical lifetime of small comets as they are scattered into the inner Solar System (*27, 32*). This requirement is consistent with modern Jupiter-family comets (JFCs), which are observed to frequently undergo spontaneous fragmentation (*33–35*), and have physical lifetimes an order of magnitude shorter than their dynamical lifetimes (*36*). The spin-up of comets to their rotational disruption limits, due to anisotropic outgassing torques, has recently emerged as a leading explanation for cometary fragmentation in the inner Solar System (*37–40*). Not only is the modern population of JFCs strongly sculpted by rotational instability (*37, 41*), but the timescale of rotational spin-up is strongly size-dependent [(*37*); see also Supplementary Text], as is required by dynamical simulations of cometary evolution (*27, 32*).

Numerical models were used to determine the effects of rotational instability on the size-

frequency distribution (SFD) of comets scattered into the inner Solar System (*42*) . The preferential disruption of small comets, due to the strong size-dependence of anisotropic outgassing torques, is found to drive order of magnitude reduction in the number of comets accreted by the early Earth. This significant decrease in Earth's overall cometary impact flux is reflected in the substantial decrease in the slope of short-period comets' SFD at small radii (Fig. 1).

The atmospheric destruction of small and oblique comets

The low density (i.e., high porosity) and weak mechanical strength of comets (*43*) combine such that comets are particularly vulnerable to destruction during atmospheric passage – a consequence of the rapid, and violent transfer of comets' momentum to the surrounding atmosphere (*25, 44*). This is expected to be most significant for small and oblique comets, which must survive passage through comparatively massive atmospheric columns, leading to the destruction of even km-scale comets (*25*). Earth's atmosphere therefore acts as a filter – preferentially destroying small and oblique comets – and thus, biasing the population of comets able to deliver prebiotic feedstock molecules to local surficial environments.

To determine the effects of atmospheric entry on the cometary impact flux reaching Earth's surface, we use the ATMOSENTRY code (*25*) to model the deceleration and fragmentation of comets during passage through Earth's atmosphere. As discussed in Anslow et al. (*25*), a key environmental parameter controlling the survival of comets is atmospheric surface pressure. Geological constraints on the Hadean atmosphere are, however, scarce and remain subject to debate (*45*). We therefore adopt a 1 bar atmosphere, which we expect to present a best-case scenario for cometary survival (*42*).

As anticipated, the effects of atmospheric entry are most pronounced, on a population level, for small comets with initially oblique entry angles (Fig. 2). Comets smaller than $\sim$ 100 m, regardless of impact angle, are found to catastrophically fragment in explosive airbursts at high altitude, distributing their feedstock molecules over a large surface area. This represents a critical challenge for the successful delivery of prebiotic feedstock molecules, given that atmospheric entry biases the surviving population of comets against oblique impacts – the small subset of comets able to deliver their prebiotic feedstock molecules, in high concentration, to Earth's surface (*20, 22*). Conversely, a by-product of atmospheric aerobraking is the production of a low velocity tail in the comets' impact

velocity distribution, which is found to extend significantly below Earth's escape velocity. This, in contrast, will promote the intact delivery of fragile cometary organics (*20, 22*). Atmospheric entry thus not only limits the total number, but also significantly biases the distribution of comets reaching Earth's surface intact, with significant implications for the subsequent survival of prebiotic feedstock molecules during hypervelocity impact.

The inefficient delivery of prebiotic feedstock molecules to the early Earth

To assess the ability of comets to deliver, intact, prebiotic feedstock molecules to Earth's surface, we employ Monte Carlo simulation, leveraging the recent advances in short-period comet formation and evolution, and modelling of cometary atmospheric entry described thus far.

We discretise Earth's cometary bombardment into 1 Myr time bins, generating the population of comets incident at the top-of-atmosphere from a Poisson distribution with mean number anchored to the Nesvorný et al. (*26*) impact chronology [see (*42*) for more details]. The population of comets (and fragments thereof) reaching Earth's surface intact, surviving atmospheric entry, is determined using the numerical model ATMOSENTRY as described above. For each comet reaching the surface, the amount of HCN surviving the high-temperature conditions associated with hypervelocity impact is finally calculated following McDonald et al. (*22*).

Our simulations record the total mass accretion of $(2.63 \pm 0.19) \times 10^{18}$ kg, which is consistent with constraints on total cometary accretion from noble gas isotopic ratios [$\sim 10^{18}$ kg; (*46, 47*)], lending independent support to our parametrised model of Earth's cometary bombardment. Yet, stringent constraints on comet size and entry angle – required for the survival of comets during atmospheric entry – are largely in tension with the survival of HCN during cometary impact (*22, 25*). The successful delivery of HCN is accordingly limited to a very narrow region of parameter space (Supplementary Text), which as we show below, renders comets an insignificant source of concentrated HCN on both global and local scales.

On a global scale we find, in agreement with the results of Todd & Öberg (*21*), that comets are unable to deliver a prebiotically relevant concentration of HCN to the early Earth. Cumulative, intact, HCN delivery is limited to only 2.65×10^{13} kg. Diluted in 1 terrestrial ocean of water – totally neglecting the subsequent hydrolysis and degradation of HCN – this corresponds to a maximum

concentration of $\sim 0.75\ \mu$M, which is orders of magnitude below that used in prebiotic experiment. Alternatively, assuming a 1 bar N_2-dominated atmosphere, this corresponds to a maximum HCN mixing ratio of order 10^{-6} – several orders of magnitude below that possible via photochemistry in both neutral (*9*) and transiently reducing (*12, 13*) atmospheres.

The potential role of comets in the origins of life on Earth is therefore restricted to the delivery of HCN, in high concentration, to local subaerial environments. During our Monte Carlo simulations of Earth's cometary bombardment, we thus record the maximum concentration of HCN delivered per cometary impact – under the assumption of dilution in only the comet's water ice. This represents a significant upper limit on actual HCN concentration – and thus best-case scenario for subsequent prebiotic chemistry – given that several environmental processes will act, quickly, to dilute cometary HCN. In addition to precipitation, the thermobaric phase of impact cratering will unavoidably disrupt the local hydrosphere (or cryosphere) (*48*). A salient outcome of high-velocity cometary impacts, irrespective of the delivery of HCN, is thus the rapid influx of local groundwater into the newly-formed crater-lake, rapidly diluting surviving cometary HCN below prebiotically relevant concentrations.

To obtain meaningful results, given uncertainty in the extent of subaerial land on the early Earth (*49*), we adopt the McCulloch & Bennett (*50*) model of continental growth as a proxy for exposed landmass (following (*51*)). This is likely a significant overestimate of exposed landmass on the Hadean Earth, given the non-monotonic history of ocean volume (*52*). Indeed, it is plausible that all continental crust will have been submarine during the early Hadean – during which period Earth's cometary bombardment was most intense – limiting exposed landmass to hotspot oceanic islands (*49,53*). This is not a problem for the purposes of this work: by adopting an optimistic model of continental growth, and analogously by recording the maximum HCN concentration post-impact, we ensure our results constitute a best-case scenario for cometary delivery.

Despite representing a best-case scenario for cometary delivery, our Monte Carlo simulations of Earth's early cometary bombardment record, on average, only one cometary impact delivering a prebiotically relevant concentration of HCN (> 10 mM); 28 % of simulations record no successful impact at all. This reflects significant inefficiency in the delivery of HCN, given that Earth accreted more than 10^5 ($D > 100$ m) comets during this early period of intense impact bombardment. This inefficiency is driven primarily by the high characteristic impact velocity of short-period

comets (*26*), which is found to restrict the successful delivery of HCN to only highly-oblique impacts at the low-velocity tail of the comets' impact velocity distribution (Supplementary Text). This corresponds to a very small region of parameter space, which is only sampled at very early times when the cometary impact flux is highest (Fig. 3). Consequently, the most probable timing of successful cometary impact is in the early Hadean, $4.46^{+0.07}_{-0.26}$ Gya, more than 100 Myr earlier than the estimated emergence of the last universal common ancestor (LUCA) at ~ 4.2 Gya (*54*).

The inability of comets to robustly deliver HCN in high concentration is further compounded by the coincidence of Earth's most intense cometary bombardment with the limited availability of exposed subaerial land during the early Hadean (*49, 52*). Owing to the near absence of continental crust during the early Hadean (*49*), our simulations record a significant number of low-velocity cometary impacts onto Earth's early oceans. Any surviving HCN from these impacts will have been quickly diluted and lost to hydrolysis, unable to trigger subsequent prebiotic chemistry. Taken together, our results demonstrate that restrictions on comet size, velocity, and angle – imposed by constraints on the survival of comets and their HCN during impact with Earth – combine such that the successful delivery of prebiotic feedstock molecules was an exceedingly rare event, limited in this best-case scenario to a single cometary impact.

Comparative analysis of inner Solar System cometary bombardment

Despite lacking any evidence of life, the dynamical simulations of Nesvorný et al. (*26*) allow us to also consider the prebiotic implications of this early period of cometary bombardment for Mars and Venus, our closest planetary neighbours. Given sparse paleoenvironmental constraints for both Mars and Venus, we adopt modern-day environmental parameters to enable direct comparison with Earth. Critically, despite abundant geological evidence of fluvial processes on Mars (*55, 56*), the nature and evolution of surficial water on Mars remain subject to debate, while more fundamental uncertainty remains regarding the existence of liquid-water oceans on Venus (*57–59*). Accordingly, we make no assumption regarding the extent of subaerial landmass, and focus only on the cometary flux surviving atmospheric entry, and HCN surviving hypervelocity impact.

We find that cometary delivery is far more effective onto Mars (Fig. 4). Despite an overall impact flux ~ 5× lower than on Earth and Venus (*26*), Mars receives 1061 ± 32 impacts delivering

$>$ 10 mM HCN, compared with 189 ± 13 for Earth (ignoring the extent of subaerial landmass) and 53 ± 7 for Venus. This efficiency is driven primarily by lower cometary impact velocities – a consequence of Mars' lower escape velocity and larger semi-major axis (*60*) – and Mars' tenuous atmosphere. These combine such that almost all $D > 100$ m comets are able to survive atmospheric entry (Fig. 2), with a much larger fraction of these comets delivering their HCN intact. Even if Mars' early atmospheric surface pressure approached 1 bar, to facilitate stable surface liquid water (*61*), the number of successful impacts (657 ± 25) remains more than three times greater than on Earth. In stark contrast, Venus' dense atmosphere destroys the majority of incident comets – even those several kilometres in diameter – making the successful delivery of HCN substantially more challenging than onto Earth.

This simple comparison between the Solar System's terrestrial planets suggests that, all else being equal, Mars would have been the more favourable target for the cometary delivery of prebiotic feedstock molecules, and if cometary delivery is an important prerequisite step for prebiotic chemistry, strengthens the possibility that life could have emerged on Mars. We caution, however, that this analysis is agnostic to global environmental conditions, including most importantly the availability of subaerial land, and thus reiterate that these results represent a best case scenario for subsequent prebiotic chemistry. Indeed, the dearth of exposed land on the Hadean Earth decreases the number of successful impacts from 189 to only 1. Clearly, a similar reduction might also be realised in the case of a warm and wet (pre-)Noachian Mars, harbouring a globally significant reservoir of surficial water.

Discussion

Implications for the origins of life on Earth

Although Solar System comets boast a rich diversity of volatile organic species – including crucially many prebiotic feedstock molecules in high concentration (*17*) – we have shown via Monte Carlo simulation of Earth's cometary bombardment that these comets were, on the whole, unable to deliver these fragile organic molecules to Earth's surface intact. Our results demonstrate that, on both global and local scales, cometary impacts provided an insignificant source of the concentrated

feedstock molecules required for prebiotic chemistry, challenging the long-held hypothesis that comets played an important role in the origins of life on Earth (*14, 15, 18–20*).

On a global scale, the intact delivery of HCN is orders of magnitude below what can be produced endogenously in even the most unfavourable (i.e., oxidising) atmospheric conditions. On a local scale, we find that in the best-case scenario, the delivery of a prebiotically relevant concentration of HCN is limited to, on average, one impact occurring at $4.46^{+0.07}_{-0.26}$ Gya (Fig. 3). These results reflect the rapid decline in Earth's cometary bombardment (*26*), the limited availability of subaerial land (*49*), and the exceedingly small region of parameter space in which HCN can survive hypervelocity impact (*22*).

Multiple lines of evidence suggest that these results represent a best-case scenario for the cometary delivery of HCN, and indeed other prebiotic feedstock molecules. Most significantly, whenever faced with loosely constrained environmental parameters throughout our analysis – such as atmospheric surface pressure or the extent of subaerial land on the Hadean Earth – we have adopted values (within plausible limits) to maximise the number of successful cometary impacts. Moreover, it is likely that we significantly overestimate HCN survival during cometary impacts. We adopt a parametrised model of HCN survival directly from McDonald et al. (*22*), which is based on idealised simulations that include only one destruction pathway for HCN, and crucially, neglect comets' internal strength and porosity – both of which are expected to increase peak temperatures during hypervelocity impact.

It is therefore overwhelmingly likely, based on the results of our Monte Carlo simulations, that in practice no comets delivered a prebiotically relevant concentration of HCN, in tension with the long-held hypothesis that cometary impacts may have played an important role in the origins of life on Earth (*14, 15, 18–20*). Nonetheless, we cannot discount the possibility – in the spirit of Clark (*18*) – that during the early Hadean, the fortuitous collision of a low-velocity, highly oblique comet may have delivered almost all of its HCN intact. It is therefore critical to address the additional environmental barriers that subsequent prebiotic chemistry would face in the event of such a stochastic, successful cometary impact.

The most immediate and decisive threat to subsequent prebiotic chemistry is the environmental dilution of cometary HCN. During hypervelocity impact, a comet's kinetic energy is rapidly transferred to the Earth, with peak pressures of order 10 – 100 GPa driving the shock metamorphism

(fracture, deformation and melting) of target rocks (*62*). A significant outcome of this initial and violent 'thermobaric' phase of impact cratering is the disruption of the local hydrosphere (or cryosphere) (*48*). On a timescale of only days to weeks, the influx of local groundwater into the newly-formed impact crater, coupled with routine precipitation and surficial runoff, will act to rapidly dilute cometary HCN. Further compounded by the subsequent hydrolysis of HCN into formamide (*21*), even an initially prebiotically competitive concentration of HCN will be quickly driven below functional levels.

Subsequent prebiotic chemistry must therefore succeed on short timescale, while cometary HCN remains at a prebiotically functional concentration. As we will now demonstrate, this places strict – and, we argue, implausible – constraints on the efficiency of prebiotic chemistry, challenging the long-held suggestion that comets played an important role in the origins of life on Earth.

To place this on a quantitative footing, we make the simplifying assumption that a successful cometary impact is a necessary prerequisite step for the origins of life. Given that a single cometary impact will never deliver the full complement of bioessential feedstock molecules required for any prebiotic chemical network, we further assume there is some (unknown) probability of abiogenesis per unit time, $p_{\rm abio}$. If prebiotic chemistry can only occur within $\tau_{\rm HCN}$ of successful cometary impact – i.e., the time window during which HCN remains in sufficiently high concentration – then the probability this chemistry succeeds following a single cometary impact is thus

$$p_{\rm suc} = 1 - \exp\left(-p_{\rm abio}\tau_{\rm HCN}\right) \simeq p_{\rm abio}\tau_{\rm HCN}, \tag{1}$$

assuming $p_{\rm abio}\tau_{\rm HCN} \ll 1$.

Given that our Monte Carlo simulations reveal that the successful cometary delivery of HCN was an exceedingly rare event, we are able to estimate the likelihood of prebiotic chemistry succeeding on the early Earth. Specifically, we derive a heuristic origins of life timescale, $\tau_{\rm ool}$, representing the expected time required for prebiotic chemistry to succeed given both the rarity of successful cometary impact, and the rapid environmental dilution of cometary HCN. If this timescale is significantly longer than the duration of Earth's intense cometary bombardment, this would quantitatively encode how unlikely it is that cometary impacts played an important role in the origins of life on Earth.

The results of our Monte Carlo simulations demonstrate – if they occurred at all – that successful

cometary impacts are overwhelmingly likely to have occurred early in Earth's history, with less than 5 % of simulations recording the successful delivery of HCN later than 4.00 Gya (Fig. 3). To first order, the number of successful impacts can be modelled as Bernoulli distributed with constant rate $r_{\rm imp} = T_{\rm imp}^{-1} \sim 2 \times 10^{-3}$ Myr^{-1}, where $T_{\rm imp} \simeq 500$ Myr is the approximate duration of Earth's intense cometary bombardment. This heuristic origins of life timescale is thus given by

$$\tau_{\rm ool} \simeq \lambda_{\rm suc}^{-1} \simeq \frac{T_{\rm imp}}{p_{\rm abio}\tau_{\rm HCN}}, \tag{2}$$

which is shown in Fig. 5 across a wide range of $p_{\rm abio} - \tau_{\rm HCN}$ parameter space. In the following paragraphs, we constrain plausible bounds for $\tau_{\rm HCN}$ and $p_{\rm abio}$, thereby allowing this illustrative calculation to quantitatively assess the potential role of cometary impacts in the origins of life on Earth.

As already discussed, there are several competing environmental and chemical processes that, together, will control the productive lifetime of a cometary crater-lake, $\tau_{\rm HCN}$. Of these, we expect the environmental dilution of cometary HCN to play the most decisive role, operating on a timescale of days to weeks following cometary impact (*48*). If, however, supportive environmental conditions prevent the rapid dilution of HCN, the residence time of the crater-lake – the average time water remains in the lake – would instead be the more appropriate timescale to consider. Through analogy with modern lakes, we expect this timescale to be of the order $1 - 10$ yr (*63*). Thus, while the hydrolysis of HCN into formamide will occur over much longer timescales ($\gtrsim$ kyr), dependent on both temperature and pH (*64*), it is highly unlikely that appreciable cometary HCN will survive long enough for this to represent a dominant loss process.

Under the assumption that a successful cometary impact is a necessary prerequisite step for the origins of life, $p_{\rm abio}$ is conceptually equivalent to the abiogenesis rate adopted and discussed in (*65, 66*). These Bayesian analyses, conditioned upon the early emergence of life on Earth, support an abiogenesis rate in the approximate range $10^{-3} < p_{\rm abio} < 10^{3}$ Gyr^{-1} (*65, 66*). This would imply an origins of life timescale in excess of the age of the Universe for the plausible values of $\tau_{\rm HCN}$ considered above (Fig. 5). While it is clear that we are fundamentally limited by our ignorance regarding most inputs required to determine such a quantity, reliance on a single cometary impact, and the short time-window available for prebiotic chemistry, combine such that the results of this heuristic exercise are robust to significant uncertainty in the abiogenesis rate, $p_{\rm abio}$.

It is therefore apparent, through Monte Carlo simulation of Earth's cometary bombardment, that synthetic prebiotic chemistry was exceedingly unlikely to succeed following cometary impact. While cometary HCN could, in principle, be subsequently concentrated and stored in ferrocyanide salts (*1*), it is non-trivial to subsequently release this cyanide in a reactive form (*67*). This would likely require the thermal transformation of ferrocyanide salts via volcanism or lightning, introducing an additional reliance on supportive local environmental conditions to what is already a quantitatively implausible scenario. Moreover, this would remove the principal advantage attributed to cometary delivery – the immediate delivery of a prebiotically relevant concentration of key feedstock molecules – and so confers little benefit relative to an endogenous source of these molecules. Despite not reaching concentrations immediately comparable to that used in prebiotic experiment (*12, 13, 68*), an endogenous source would by contrast deliver these key feedstock molecules, in quasi steady-state, to all exposed subaerial land.

To summarise, our results demonstrate that Earth's cometary bombardment was unable to provide the concentrated reservoir of bioessential feedstock molecules required for synthetic prebiotic chemistry, challenging the long-held suggestion that cometary impacts may plausibly have played an important role in the origins of life on Earth. While we cannot formally exclude the possibility that a single fortuitous cometary impact delivered a prebiotically plausible concentration of HCN, we have demonstrated this would impose strict – and, we argue, implausible – constraints on the efficiency of subsequent prebiotic chemistry. Prebiotic chemistry would be required to succeed on short timescales, before the rapid environmental dilution of exogenous feedstock molecules, in the handful of local environments afforded by a single cometary impact.

Prospects for cometary delivery beyond Earth

While our results demonstrate that cometary impacts were exceedingly unlikely to have played an important role in the origins of life on Earth – the only known instance of life – we find that cometary impacts will more readily deliver HCN, in high concentration, to Mars. Farther afield, many exoplanetary systems harbour large outer reservoirs of icy planetesimals in debris disks analogous to the Kuiper belt – with many inferred to have masses 6 orders of magnitude larger (*69*). Our results therefore clearly cannot preclude the possibility that, in favourable planetary contexts,

cometary delivery may provide a robust source of concentrated prebiotic feedstock molecules. Here, we discuss the implications of our results for the prospects of cometary delivery beyond Earth.

Comparison of the end-member cases of Mars and Venus, enabled by their shared dynamical origins, highlights several key planetary and planetary system requirements that control the efficiency, and thus importance, of cometary delivery in a general exoplanetary context. The significant differences between Mars and Venus are driven by atmospheric surface density, and the impact velocity distribution of short-period comets. The destruction of almost all comets smaller than 2 km during descent through Venus' dense atmosphere, compounded by an average cometary impact velocity greater than 36 $\mathrm{km\,s^{-1}}$ (*26*), restricts successful cometary delivery to an extremely small region of impact parameter space [(*22*), Supplementary Text]. Mars, in contrast, benefits from its tenuous atmosphere that allows almost all ($D < 100$ m) comets to reach the surface intact with an average impact velocity of only 19.7 $\mathrm{km\,s^{-1}}$ (*26*), which together supports the successful delivery of HCN in a much larger fraction of cometary impacts.

Given that the detailed atmospheric characterisation of terrestrial exoplanets remains elusive [e.g., (*70*)], the key observationally accessible planetary property controlling the efficiency of cometary delivery is thus planet size. Current observational biases skew the present-day exoplanet population preferentially towards larger planets, such that well-characterised escape velocities are consistently, and substantially higher than of Earth (Supplementary Text). For this reason alone, we would expect cometary delivery to be significantly more challenging for the majority of terrestrial exoplanets discovered to-date.

Constraints on the efficiency of cometary delivery at the planetary system level are less straightforward, given the large number of (relevant) free parameters that would need to be considered on a system-by-system basis. Nevertheless, a minimum prerequisite is that the inner planetary system must experience a period of intense cometary bombardment in order to overcome the very low collision probability of highly-eccentric comets onto terrestrial planets with small semi-major axis [e.g., (*26, 71*)]. Such a period of intense cometary bombardment is not, however, guaranteed in a general exoplanetary context, with the dynamical influence of exterior planets able to prevent, in the extreme case, the inwards transport of comets through the planetary system (*72*). Crucially, this is most pronounced for low-mass stars around which even Earth-mass planets have the capacity to form effective dynamical barriers (*72*).

We finally note that planetary system architecture and stellar mass both also play a significant role in determining the impact velocity distribution of comets onto terrestrial exoplanets. This is, again, most challenging around low-mass stars for which the minimum impact velocity of short-period comets is significantly higher than around Solar-type stars (*60*). This represents a significant, additional problem for cometary delivery given that the majority of Earth-like planets amenable to detailed atmospheric characterisation in the coming decades orbit low-mass M-dwarf stars – the so-called "M-dwarf opportunity" (*73*).

It therefore appears overwhelmingly likely that cometary delivery will be substantially more challenging in a general exoplanetary context than onto Earth, driven by much higher characteristic cometary impact velocities and the efficient destruction of fragile prebiotic feedstock molecules. Taken together with our central result – that Earth's cometary bombardment was unable to provide the concentrated reservoir of prebiotic feedstock molecules required for the origins of life – we expect the same to be true in a general exoplanetary context, challenging the long-held hypothesis that cometary impacts are likely to play an important role in the origins of life.

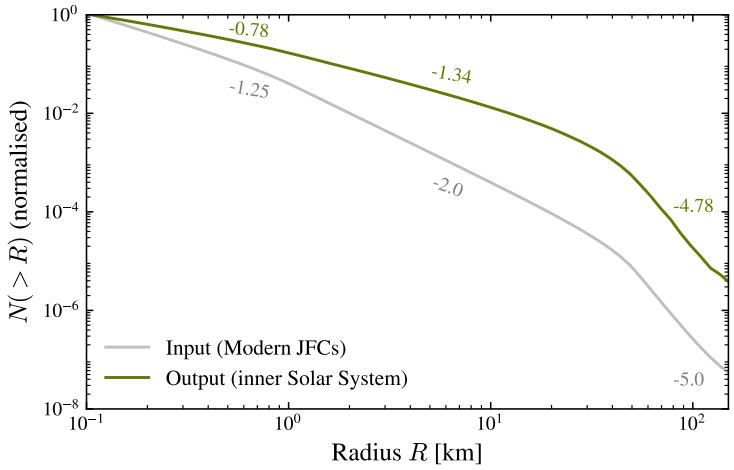

Figure 1: **Cumulative size-frequency distribution (SFD) of comets entering the inner Solar System subject to disruption via rotational instability.** The slopes of the input (gray) and output (green) SFDs are annotated next to the curves for the size ranges 0.1 – 1 km, 1 – 50 km, and 50 – 150 km. The strong size-dependence of rotational spin-up (*37*) drives the preferential disruption of small comets, causing a significant decrease in the power-law slope at small radii.

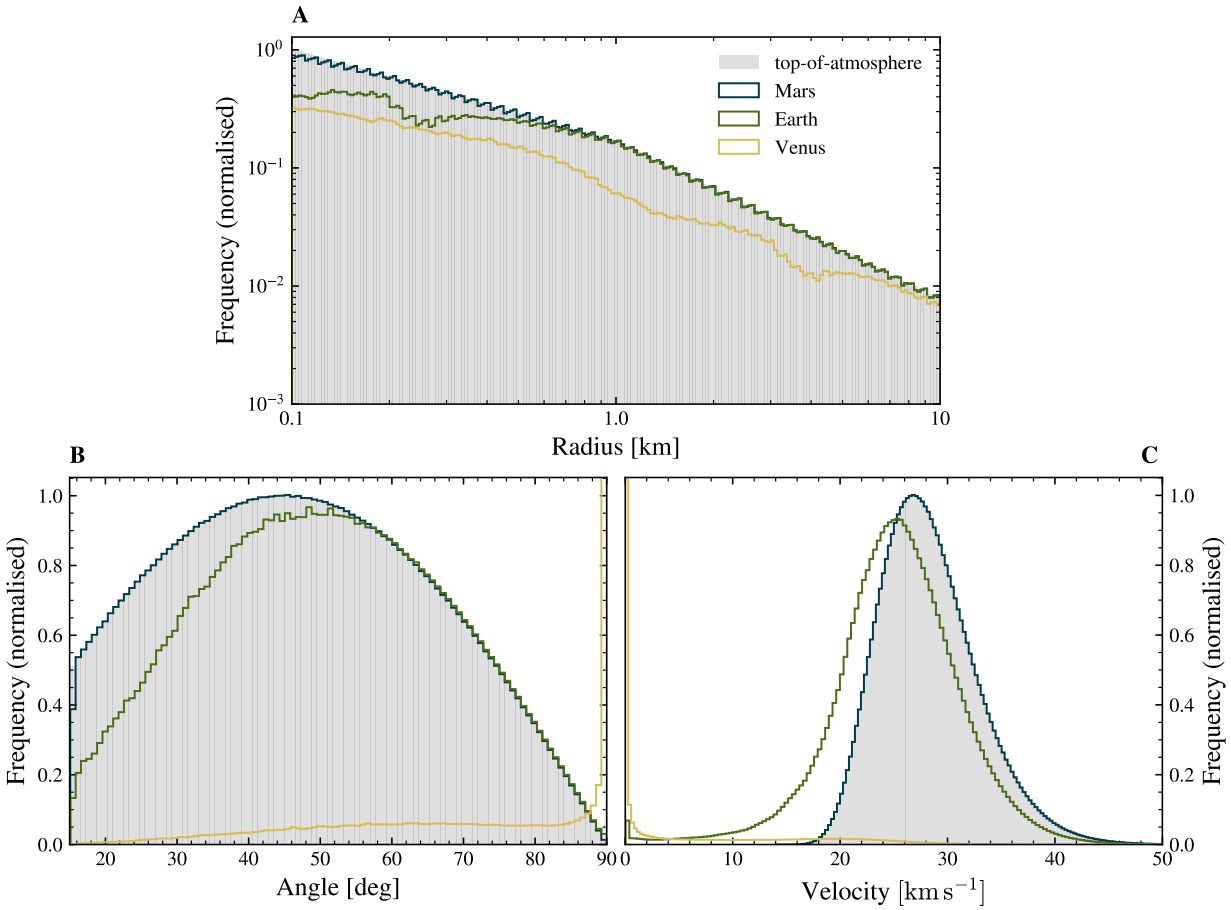

Figure 2: **The influence of atmospheric entry on short-period comets' size, impact angle and impact velocity distributions.** The gray shaded histograms show the initial size (**A**), angle (**B**), and velocity (**C**) distributions of comets incident at the top of Earth's atmosphere. The corresponding distributions following atmospheric entry are shown for modern-day terrestrial (green), Martian (blue) and Venusian (yellow) atmospheres.

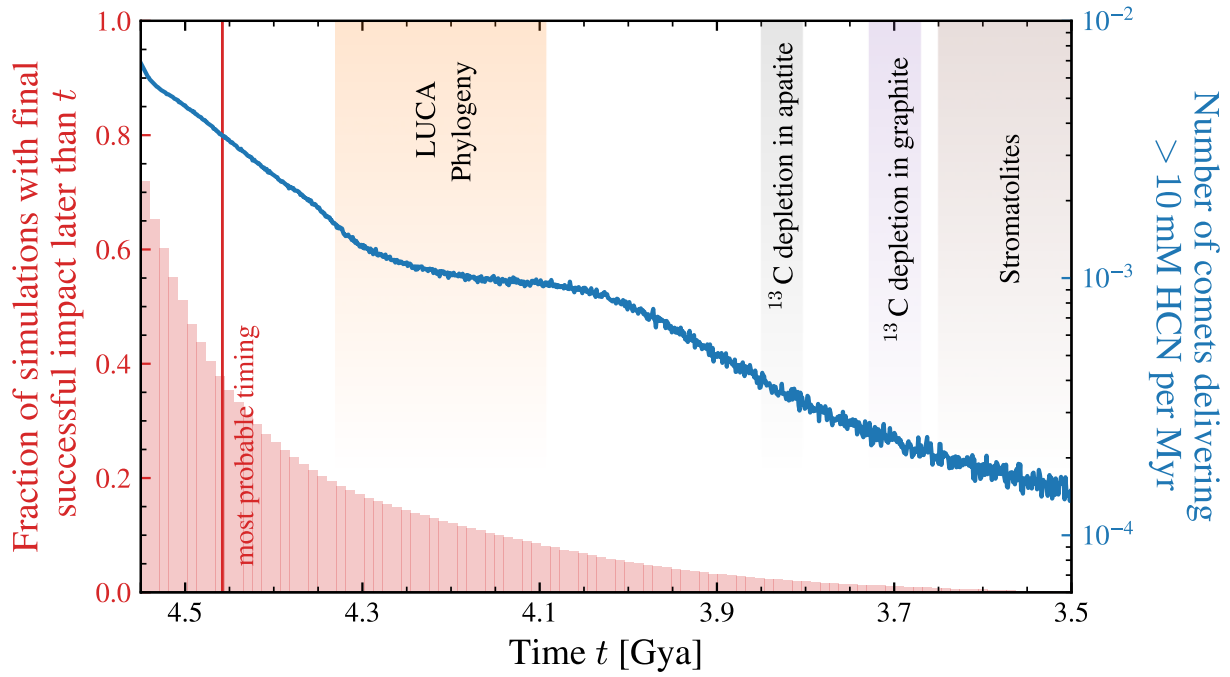

Figure 3: **Results from 100,000 Monte Carlo realisations of Earth's cometary bombardment history.** The number of comets delivering a prebiotically relevant concentration ($\geq$ 10 mM) of HCN per 1 Myr time-bin, following the Nesvorný et al. (*26*) impact chronology, is shown in blue. We consider only cometary impacts onto exposed subaerial land and use the McCulloch & Bennett (*50*) model of continental growth [see (*42*)]. The median number of successful cometary impacts per Monte Carlo realisation is only 1, with 28 % of our simulations recording no successful cometary impact. Successful cometary impacts are overwhelmingly likely to occur early in Earth's history (shown in red), with less than 5% of our simulations recording the delivery of $>$ 10 mM HCN later than 4.00 Gya. The most probable timing of successful cometary impact is $4.46^{+0.07}_{-0.26}$ Gya – more than 100 Myr earlier than the first, indirect evidence of life on Earth.

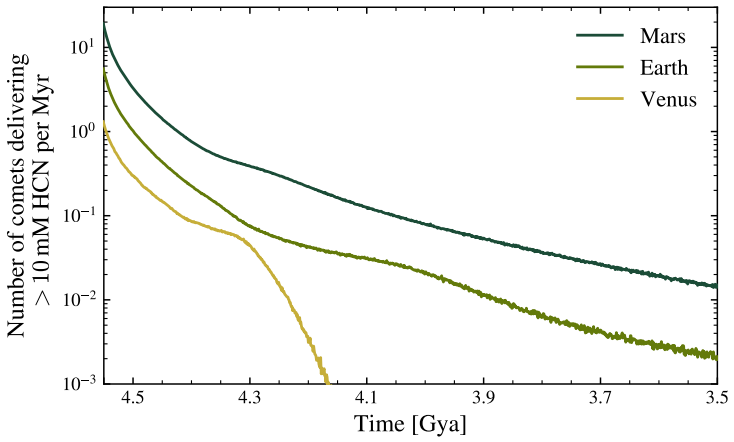

Figure 4: **Results from Monte Carlo simulations of the early cometary bombardment of Mars (blue), Earth (green) and Venus (yellow).** The number of cometary impacts delivering a prebiotically relevant concentration (> 10 mM) of HCN as a function of time, in bins of 1 Myr, averaged over 10^5 Monte Carlo realisations of the Nesvorný (*26*) impact chronology. These results represent an upper limit on the number of environments able to support subsequent prebiotic chemistry, making no assumption about the availability of subaerial landmass.

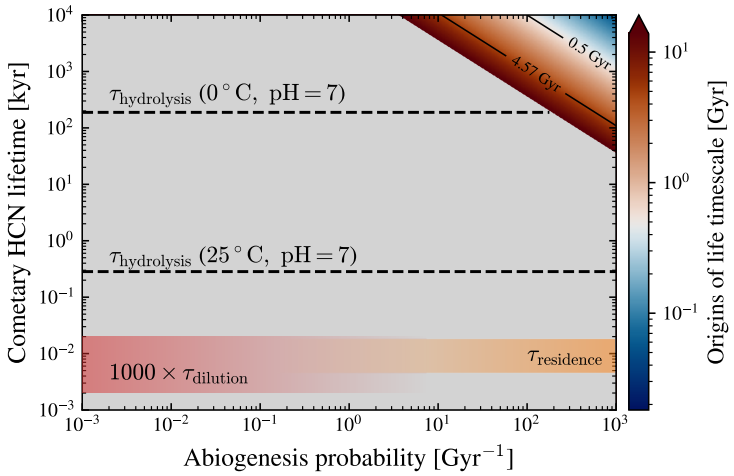

Figure 5: **The origins-of-life timescale is in excess of the age of the Solar System for plausible values of abiogenesis probability and cometary HCN lifetime.** A heuristic origins-of-life timescale, $\tau_{\rm ool}$, is calculated under the assumption that a successful cometary impact is a necessary prerequisite for the origins of life. Bayesian analyses, conditioned on the early emergence of life on Earth, support an abiogenesis probability in the range $10^{-3} < p_{\rm abio} < 10^{3}$ Gyr^{-1} (*65, 66*). The lifetime of cometary HCN is expected to be determined by either the timescale of environmental dilution [(*48*), red horizontal band], or the residence time of the crater-lake [(*63*), orange horizontal band]. The hydrolysis lifetime of HCN in aqueous solution at 0°C and 25°C [(*64*), black dashed lines] represent significant upper limits. In all cases, this heuristic origins-of-life timescale is orders of magnitude larger than the duration of Earth's intense cometary bombardment: prebiotic chemistry was exceedingly unlikely to succeed following successful cometary impact.

References and Notes

1. D. D. Sasselov, J. P. Grotzinger, J. D. Sutherland, The origin of life as a planetary phenomenon. *Science Advances* **6** (6), eaax3419 (2020), doi:10.1126/sciadv.aax3419.

2. M. W. Powner, B. Gerland, J. D. Sutherland, Synthesis of activated pyrimidine ribonucleotides in prebiotically plausible conditions. *Nature* **459** (7244), 239–242 (2009), doi:10.1038/nature08013.

3. B. H. Patel, C. Percivalle, D. J. Ritson, C. D. Duffy, J. D. Sutherland, Common origins of RNA, protein and lipid precursors in a cyanosulfidic protometabolism. *Nature Chemistry* **7** (4), 301–307 (2015), doi:10.1038/nchem.2202.

4. S. Becker, J. Feldmann, S. Wiedemann, H. Okamura, C. Schneider, K. Iwan, A. Crisp, M. Rossa, T. Amatov, T. Carell, Unified prebiotically plausible synthesis of pyrimidine and purine RNA ribonucleotides. *Science* **366** (6461), 76–82 (2019), doi:10.1126/science.aax2747.

5. J. Xu, D. J. Ritson, S. Ranjan, Z. R. Todd, D. D. Sasselov, J. D. Sutherland, Photochemical reductive homologation of hydrogen cyanide using sulfite and ferrocyanide. *Chem. Commun.* **54**, 5566–5569 (2018), doi:10.1039/C8CC01499J, `http://dx.doi.org/10.1039/C8CC01499J`.

6. C. S. Foden, S. Islam, C. Fernández-García, L. Maugeri, T. D. Sheppard, M. W. Powner, Prebiotic synthesis of cysteine peptides that catalyze peptide ligation in neutral water. *Science* **370** (6518), 865–869 (2020), doi:10.1126/science.abd5680.

7. C. Chyba, C. Sagan, Endogenous production, exogenous delivery and impact-shock synthesis of organic molecules: an inventory for the origins of life. *Nature* **355** (6356), 125–132 (1992), doi:10.1038/355125a0.

8. K. J. Zahnle, Photochemistry of methane and the formation of hydrocyanic acid (HCN) in the Earth's early atmosphere. *Journal of Geophysical Research: Atmospheres* **91** (D2), 2819–2834 (1986), doi:10.1029/JD091iD02p02819.

9. P. B. Rimmer, S. Rugheimer, Hydrogen cyanide in nitrogen-rich atmospheres of rocky exoplanets. *Icarus* **329**, 124–131 (2019), doi:10.1016/j.icarus.2019.02.020.

10. S. Aulbach, V. Stagno, Evidence for a reducing Archean ambient mantle and its effects on the carbon cycle. *Geology* **44** (9), 751–754 (2016), doi:10.1130/G38070.1.

11. D. C. Catling, J. F. Kasting, *Atmospheric Evolution on Inhabited and Lifeless Worlds* (2017).

12. K. J. Zahnle, R. Lupu, D. C. Catling, N. Wogan, Creation and Evolution of Impact-generated Reduced Atmospheres of Early Earth. *Planet. Sci. J.* **1** (1), 11 (2020), doi:10.3847/PSJ/ab7e2c.

13. N. F. Wogan, D. C. Catling, K. J. Zahnle, R. Lupu, Origin-of-life Molecules in the Atmosphere after Big Impacts on the Early Earth. *Planet. Sci. J.* **4** (9), 169 (2023), doi:10.3847/PSJ/aced83.

14. T. C. Chamberlin, R. T. Chamberlin, Early Terrestrial Conditions That May Have Favored Organic Synthesis. *Science* **28** (730), 897–911 (1908), doi:10.1126/science.28.730.897.

15. J. Oró, Comets and the Formation of Biochemical Compounds on the Primitive Earth. *Nature* **190** (4774), 389–390 (1961), doi:10.1038/190389a0.

16. S. J. Clemett, C. R. Maechling, R. N. Zare, P. D. Swan, R. M. Walker, Identification of Complex Aromatic Molecules in Individual Interplanetary Dust Particles. *Science* **262** (5134), 721–725 (1993), doi:10.1126/science.262.5134.721.

17. M. J. Mumma, S. B. Charnley, The Chemical Composition of Comets—Emerging Taxonomies and Natal Heritage. *Annual Review of Astronomy and Astrophysics* **49** (1), 471–524 (2011), doi:10.1146/annurev-astro-081309-130811.

18. B. C. Clark, Primeval procreative comet pond. *Origins of life and evolution of the biosphere* **18** (3), 209–238 (1988), doi:10.1007/BF01804671.

19. C. F. Chyba, P. J. Thomas, L. Brookshaw, C. Sagan, Cometary Delivery of Organic Molecules to the Early Earth. *Science* **249** (4967), 366–373 (1990).

20. E. Pierazzo, C. F. Chyba, Amino acid survival in large cometary impacts. *Meteoritics & Planetary Science* **34** (6), 909–918 (1999), doi:10.1111/j.1945-5100.1999.tb01409.x.

21. Z. R. Todd, K. I. Öberg, Cometary Delivery of Hydrogen Cyanide to the Early Earth. *Astrobiology* **20** (9), 1109–1120 (2020), doi:10.1089/ast.2019.2187.

22. C. H. McDonald, A. Bonsor, A. S. Rae, P. B. Rimmer, R. J. Anslow, Z. R. Todd, Constraining the survival of HCN during cometary impacts. *Icarus* p. 116704 (2025), doi:https://doi.org/10.1016/j.icarus.2025.116704.

23. N. E. B. Zellner, V. P. McCaffrey, J. H. E. Butler, Cometary Glycolaldehyde as a Source of pre-RNA Molecules. *Astrobiology* **20** (11), 1377–1388 (2020), doi:10.1089/ast.2020.2216.

24. N. Hänni, K. Altwegg, H. Balsiger, M. Combi, S. A. Fuselier, J. De Keyser, B. Pestoni, M. Rubin, S. F. Wampfler, Cyanogen, cyanoacetylene, and acetonitrile in comet 67P and their relation to the cyano radical. *Astronomy & Astrophysics* **647**, A22 (2021), doi:10.1051/0004-6361/202039580.

25. R. J. Anslow, A. Bonsor, Z. R. Todd, R. Wordsworth, A. S. P. Rae, C. H. McDonald, P. B. Rimmer, The atmospheric entry of cometary impactors. *Monthly Notices of the Royal Astronomical Society* **539** (1), 376–392 (2025), doi:10.1093/mnras/staf507.

26. D. Nesvorný, F. V. Roig, D. Vokrouhlický, W. F. Bottke, S. Marchi, A. Morbidelli, R. Deienno, Early bombardment of the moon: Connecting the lunar crater record to the terrestrial planet formation. *Icarus* **399**, 115545 (2023), doi:10.1016/j.icarus.2023.115545.

27. D. Nesvorný, D. Vokrouhlický, L. Dones, H. F. Levison, N. Kaib, A. Morbidelli, Origin and Evolution of Short-period Comets. *The Astrophysical Journal* **845** (1), 27 (2017), doi:10.3847/1538-4357/aa7cf6.

28. D. Nesvorný, D. Vokrouhlický, A. S. Stern, B. Davidsson, M. T. Bannister, K. Volk, Y.-T. Chen, B. J. Gladman, J. J. Kavelaars, J.-M. Petit, S. D. J. Gwyn, M. Alexandersen, OSSOS. XIX. Testing Early Solar System Dynamical Models Using OSSOS Centaur Detections. *The Astronomical Journal* **158** (3), 132 (2019), doi:10.3847/1538-3881/ab3651.

29. M. E. Bailey, Comet craters versus asteroid craters. *Advances in Space Research* **11** (6), 43–60 (1991), doi:10.1016/0273-1177(91)90231-8.

30. N. E. B. Zellner, Cataclysm No More: New Views on the Timing and Delivery of Lunar Impactors. *Origins of Life and Evolution of the Biosphere* **47** (3), 261–280 (2017), doi:10.1007/s11084-017-9536-3.

31. R. G. Strom, R. Malhotra, T. Ito, F. Yoshida, D. A. Kring, The Origin of Planetary Impactors in the Inner Solar System. *Science* **309** (5742), 1847–1850 (2005), doi:10.1126/science.1113544.

32. R. P. Di Sisto, J. A. Fernández, A. Brunini, On the population, physical decay and orbital distribution of Jupiter family comets: Numerical simulations. *Icarus* **203** (1), 140–154 (2009), doi:10.1016/j.icarus.2009.05.002.

33. Z. Sekanina, Disappearance and disintegration of comets. *Icarus* **58** (1), 81–100 (1984), doi:10.1016/0019-1035(84)90099-X.

34. H. Boehnhardt, Comet Splitting - Observations and Model Scenarios. *Earth Moon and Planets* **89** (1), 91–115 (2002), doi:10.1023/A:1021538201389.

35. D. Jewitt, M. Mutchler, H. Weaver, M.-T. Hui, J. Agarwal, M. Ishiguro, J. Kleyna, J. Li, K. Meech, M. Micheli, R. Wainscoat, R. Weryk, Fragmentation Kinematics in Comet 332P/Ikeya-Murakami. *The Astrophysical Journal Letters* **829** (1), L8 (2016), doi:10.3847/2041-8205/829/1/L8.

36. H. F. Levison, M. J. Duncan, From the Kuiper Belt to Jupiter-Family Comets: The Spatial Distribution of Ecliptic Comets. *Icarus* **127** (1), 13–32 (1997), doi:10.1006/icar.1996.5637.

37. D. Jewitt, Systematics and Consequences of Comet Nucleus Outgassing Torques. *The Astronomical Journal* **161** (6), 261 (2021), doi:10.3847/1538-3881/abf09c.

38. T. K. Safrit, J. K. Steckloff, A. S. Bosh, D. Nesvorny, K. Walsh, R. Brasser, D. A. Minton, The Formation of Bilobate Comet Shapes through Sublimative Torques. *Planet Sci. J.* **2** (1), 14 (2021), doi:10.3847/PSJ/abc9c8.

39. D. Jewitt, Destruction of Long-period Comets. *The Astronomical Journal* **164** (4), 158 (2022), doi:10.3847/1538-3881/ac886d.

40. J. Luu, D. Jewitt, Continuous Fragmentation of Comet 157P/Tritton. *The Astronomical Journal* **169** (1), 14 (2024), doi:10.3847/1538-3881/ad8e62, https://dx.doi.org/10.3847/1538-3881/ad8e62.

41. R. Kokotanekova, C. Snodgrass, P. Lacerda, S. F. Green, S. C. Lowry, Y. R. Fernández, C. Tubiana, A. Fitzsimmons, H. H. Hsieh, Rotation of cometary nuclei: new light curves and an update of the ensemble properties of Jupiter-family comets. *Monthly Notices of the Royal Astronomical Society* **471** (3), 2974–3007 (2017), doi:10.1093/mnras/stx1716.

42. Materials and methods are available as supplementary material.

43. O. Groussin, N. Attree, Y. Brouet, V. Ciarletti, B. Davidsson, G. Filacchione, H. H. Fischer, B. Gundlach, M. Knapmeyer, J. Knollenberg, R. Kokotanekova, E. Kührt, C. Leyrat, D. Marshall, I. Pelivan, Y. Skorov, C. Snodgrass, T. Spohn, F. Tosi, The Thermal, Mechanical, Structural, and Dielectric Properties of Cometary Nuclei After Rosetta. *Space Science Reviews* **215** (4), 29 (2019), doi:10.1007/s11214-019-0594-x.

44. J. G. Hills, M. P. Goda, The Fragmentation of Small Asteroids in the Atmosphere. *The Astronomical Journal* **105**, 1114 (1993), doi:10.1086/116499.

45. D. C. Catling, K. J. Zahnle, The Archean atmosphere. *Science Advances* **6** (9), eaax1420 (2020), doi:10.1126/sciadv.aax1420.

46. B. Marty, K. Altwegg, H. Balsiger, A. Bar-Nun, D. V. Bekaert, J. J. Berthelier, A. Bieler, C. Briois, U. Calmonte, M. Combi, J. De Keyser, B. Fiethe, S. A. Fuselier, S. Gasc, T. I. Gombosi, K. C. Hansen, M. Hässig, A. Jäckel, E. Kopp, A. Korth, L. Le Roy, U. Mall, O. Mousis, T. Owen, H. Rème, M. Rubin, T. Sémon, C. Y. Tzou, J. H. Waite, P. Wurz, Xenon isotopes in 67P/Churyumov-Gerasimenko show that comets contributed to Earth's atmosphere. *Science* **356** (6342), 1069–1072 (2017), doi:10.1126/science.aal3496.

47. W. S. Cassata, A refined isotopic composition of cometary xenon and implications for the accretion of comets and carbonaceous chondrites on Earth. *Earth and Planetary Science Letters* **660**, 119307 (2025), doi:https://doi.org/10.1016/j.epsl.2025.119307, https://www.sciencedirect.com/science/article/pii/S0012821X25001062.

48. G. R. Osinski, C. S. Cockell, A. Pontefract, H. M. Sapers, The Role of Meteorite Impacts in the Origin of Life. *Astrobiology* **20** (9), 1121–1149 (2020), doi:10.1089/ast.2019.2203.

49. J. Korenaga, Was There Land on the Early Earth? *Life* **11** (11), 1142 (2021), doi:10.3390/life11111142.

50. M. T. McCulloch, V. C. Bennett, Evolution of the early Earth: Constraints from ^{143}Nd ^{142}Nd isotopic systematics. *Lithos* **30** (3), 237–255 (1993), doi:10.1016/0024-4937(93)90038-E.

51. B. K. D. Pearce, R. E. Pudritz, D. A. Semenov, T. K. Henning, Origin of the RNA world: The fate of nucleobases in warm little ponds. *Proceedings of the National Academy of Science* **114** (43), 11327–11332 (2017), doi:10.1073/pnas.1710339114.

52. J. L. Bada, J. Korenaga, Exposed Areas Above Sea Level on Earth ¿3.5 Gyr Ago: Implications for Prebiotic and Primitive Biotic Chemistry. *Life* **8** (4), 55 (2018), doi:10.3390/life8040055.

53. J. Korenaga, N. J. Planavsky, D. A. D. Evans, Global water cycle and the coevolution of the Earth's interior and surface environment. *Philosophical Transactions of the Royal Society of London Series A* **375** (2094), 20150393 (2017), doi:10.1098/rsta.2015.0393.

54. E. R. R. Moody, S. Álvarez-Carretero, T. A. Mahendrarajah, J. W. Clark, H. C. Betts, N. Dombrowski, L. L. Szánthó, R. A. Boyle, S. Daines, X. Chen, N. Lane, Z. Yang, G. A. Shields, G. J. Szöllősi, A. Spang, D. Pisani, T. A. Williams, T. M. Lenton, P. C. J. Donoghue, The nature of the last universal common ancestor and its impact on the early Earth system. *Nature Ecology & Evolution* **8** (9), 1654–1666 (2024).

55. M. H. Carr, Water on Mars. *Nature* **326** (6108), 30–35 (1987), doi:10.1038/326030a0.

56. S. M. McLennan, J. P. Grotzinger, J. A. Hurowitz, N. J. Tosca, The Sedimentary Cycle on Early Mars. *Annual Review of Earth and Planetary Sciences* **47**, 91–118 (2019), doi:10.1146/annurev-earth-053018-060332.

57. M. J. Way, A. D. Del Genio, N. Y. Kiang, L. E. Sohl, D. H. Grinspoon, I. Aleinov, M. Kelley, T. Clune, Was Venus the first habitable world of our solar system? *Geophysical Research Letters* **43** (16), 8376–8383 (2016), doi:10.1002/2016GL069790.

58. M. Turbet, E. Bolmont, G. Chaverot, D. Ehrenreich, J. Leconte, E. Marcq, Day-night cloud asymmetry prevents early oceans on Venus but not on Earth. *Nature* **598** (7880), 276–280 (2021), doi:10.1038/s41586-021-03873-w.

59. T. Constantinou, O. Shorttle, P. B. Rimmer, A dry Venusian interior constrained by atmospheric chemistry. *Nature Astronomy* **9**, 189–198 (2025), doi:10.1038/s41550-024-02414-5.

60. R. J. Anslow, A. Bonsor, P. B. Rimmer, Can comets deliver prebiotic molecules to rocky exoplanets? *Proc. R. Soc. Lond., A* **479** (2279), 20230434 (2023), doi:10.1098/rspa.2023.0434.

61. R. D. Wordsworth, The Climate of Early Mars. *Annual Review of Earth and Planetary Sciences* **44**, 381–408 (2016), doi:10.1146/annurev-earth-060115-012355.

62. H. J. Melosh, *Impact cratering : a geologic process* (Oxford University Press) (1989).

63. M. L. Messager, B. Lehner, G. Grill, I. Nedeva, O. Schmitt, Estimating the volume and age of water stored in global lakes using a geo-statistical approach. *Nature Communications* **7**, 13603 (2016), doi:10.1038/ncomms13603.

64. S. Miyakawa, H. James Cleaves, S. L. Miller, The Cold Origin of Life: A. Implications Based On The Hydrolytic Stabilities Of Hydrogen Cyanide And Formamide. *Origins of Life and Evolution of the Biosphere* **32** (3), 195–208 (2002), doi:10.1023/A:1016514305984.

65. D. S. Spiegel, E. L. Turner, Bayesian analysis of the astrobiological implications of life's early emergence on Earth. *Proceedings of the National Academy of Science* **109** (2), 395–400 (2012), doi:10.1073/pnas.1111694108.

66. J. Chen, D. Kipping, On the Rate of Abiogenesis from a Bayesian Informatics Perspective. *Astrobiology* **18** (12), 1574–1584 (2018), doi:10.1089/ast.2018.1836.

67. R. J. Anslow, A. Bonsor, P. B. Rimmer, A. S. P. Rae, C. H. McDonald, C. R. Walton, The plausibility of origins scenarios requiring two impactors. *Proceedings of the Royal Society of London Series A* **481**, 20240327 (2025), doi:10.1098/rspa.2024.0327.

68. S. A. Benner, E. A. Bell, E. Biondi, R. Brasser, T. Carell, H.-J. Kim, S. J. Mojzsis, A. Omran, M. A. Pasek, D. Trail, When Did Life Likely Emerge on Earth in

an RNA-First Process? *ChemSystemsChem* **2** (2), e1900035 (2020), doi:https://doi.org/10.1002/syst.201900035, https://chemistry-europe.onlinelibrary.wiley.com/doi/abs/10.1002/syst.201900035.

69. A. V. Krivov, M. C. Wyatt, Solution to the debris disc mass problem: planetesimals are born small? *Monthly Notices of the Royal Astronomical Society* **500** (1), 718–735 (2021), doi:10.1093/mnras/staa2385.

70. T. P. Greene, T. J. Bell, E. Ducrot, A. Dyrek, P.-O. Lagage, J. J. Fortney, Thermal emission from the Earth-sized exoplanet TRAPPIST-1 b using JWST. *Nature* **618** (7963), 39–42 (2023), doi:10.1038/s41586-023-05951-7.

71. R. Brasser, S. C. Werner, S. J. Mojzsis, Impact bombardment chronology of the terrestrial planets from 4.5 Ga to 3.5 Ga. *Icarus* **338**, 113514 (2020), doi:10.1016/j.icarus.2019.113514.

72. M. C. Wyatt, A. Bonsor, A. P. Jackson, S. Marino, A. Shannon, How to design a planetary system for different scattering outcomes: giant impact sweet spot, maximising exocomets, scattered discs. *MNRAS* **464** (3), 3385–3407 (2017), doi:10.1093/mnras/stw2633.

73. D. Charbonneau, D. Deming, The Dynamics-Based Approach to Studying Terrestrial Exoplanets. *arXiv e-prints* arXiv:0706.1047 (2007), doi:10.48550/arXiv.0706.1047.

74. J. K. Rigley, M. C. Wyatt, Comet fragmentation as a source of the zodiacal cloud. *Monthly Notices of the Royal Astronomical Society* **510** (1), 834–857 (2022), doi:10.1093/mnras/stab3482.

75. C. M. Rumpf, H. G. Lewis, P. M. Atkinson, Asteroid impact effects and their immediate hazards for human populations. *Geophysical Research Letters* **44** (8), 3433–3440 (2017), doi:10.1002/2017GL073191.

76. E. Drolshagen, T. Ott, D. Koschny, G. Drolshagen, A. K. Schmidt, B. Poppe, Velocity distribution of larger meteoroids and small asteroids impacting Earth. *Planetary and Space Science* **184**, 104869 (2020), doi:10.1016/j.pss.2020.104869.

77. D. W. Hughes, I. P. Williams, The velocity distributions of periodic comets and stream meteoroids. *Monthly Notices of the Royal Astronomical Society* **315** (3), 629–634 (2000), doi:10.1046/j.1365-8711.2000.03435.x.

78. E. Shoemaker, Physics and Astronomy of the Moon, in *Physics and Astronomy of the Moon*, A. Kopal, Ed. (Academic Press), pp. 283–571 (1962).

79. C. F. Chyba, P. J. Thomas, K. J. Zahnle, The 1908 Tunguska explosion: atmospheric disruption of a stony asteroid. *Nature* **361** (6407), 40–44 (1993), doi:10.1038/361040a0.

80. M. Guo, J. Korenaga, Argon constraints on the early growth of felsic continental crust. *Science Advances* **6** (21), eaaz6234 (2020), doi:10.1126/sciadv.aaz6234.

81. B. J. R. Davidsson, Tidal Splitting and Rotational Breakup of Solid Spheres. *Icarus* **142** (2), 525–535 (1999), doi:10.1006/icar.1999.6214.

82. B. J. R. Davidsson, Tidal Splitting and Rotational Breakup of Solid Biaxial Ellipsoids. *Icarus* **149** (2), 375–383 (2001), doi:10.1006/icar.2000.6540.

83. Z. Sekanina, Formation and Evolution of the Stream of SOHO Kreutz Sungrazers. II. Results and Implications of Monte Carlo Simulation. *arXiv e-prints* arXiv:2404.00887 (2024), doi: 10.48550/arXiv.2404.00887.

84. B. D. Warner, A. W. Harris, P. Pravec, The asteroid lightcurve database. *Icarus* **202** (1), 134–146 (2009), doi:10.1016/j.icarus.2009.02.003.

85. N. Attree, O. Groussin, L. Jorda, D. Nébouy, N. Thomas, Y. Brouet, E. Kührt, F. Preusker, F. Scholten, J. Knollenberg, P. Hartogh, H. Sierks, C. Barbieri, P. Lamy, R. Rodrigo, D. Koschny, H. Rickman, H. U. Keller, M. F. A'Hearn, A. T. Auger, M. A. Barucci, J. L. Bertaux, I. Bertini, D. Bodewits, S. Boudreault, G. Cremonese, V. Da Deppo, B. Davidsson, S. Debei, M. De Cecco, J. Deller, M. R. El-Maarry, S. Fornasier, M. Fulle, P. J. Gutiérrez, C. Güttler, S. Hviid, W. H. Ip, G. Kovacs, J. R. Kramm, M. Küppers, L. M. Lara, M. Lazzarin, J. J. Lopez Moreno, S. Lowry, S. Marchi, F. Marzari, S. Mottola, G. Naletto, N. Oklay, M. Pajola, I. Toth, C. Tubiana, J. B. Vincent, X. Shi, Tensile strength of 67P/Churyumov-Gerasimenko nucleus material from overhangs. *Astronomy & Astrophysics* **611**, A33 (2018), doi:10.1051/0004-6361/201732155.

86. R. P. Binzel, S. Xu, S. J. Bus, E. Bowell, Origins for the Near-Earth Asteroids. *Science* **257** (5071), 779–782 (1992), doi:10.1126/science.257.5071.779.

87. F. L. Whipple, A comet model. I. The acceleration of Comet Encke. *The Astrophysical Journal* **111**, 375–394 (1950), doi:10.1086/145272.

88. B. G. Marsden, Z. Sekanina, D. K. Yeomans, Comets and nongravitational forces. V. *The Astronomical Journal* **78**, 211 (1973), doi:10.1086/111402.

89. D. Jewitt, Cometary Rotation: an Overview. *Earth Moon and Planets* **79**, 35–53 (1997), doi:10.1023/A:1006272914117.

90. N. H. Samarasinha, B. E. A. Mueller, Relating Changes in Cometary Rotation to Activity: Current Status and Applications to Comet C/2012 S1 (ISON). *The Astrophysical Journal Letters* **775** (1), L10 (2013), doi:10.1088/2041-8205/775/1/L10.

91. R. R. Rafikov, Non-Gravitational Forces and Spin Evolution of Comets. *arXiv e-prints* arXiv:1809.05133 (2018), doi:10.48550/arXiv.1809.05133.

92. R. Kokotanekova, C. Snodgrass, P. Lacerda, S. F. Green, P. Nikolov, T. Bonev, Implications of the small spin changes measured for large Jupiter-family comet nuclei. *Monthly Notices of the Royal Astronomical Society* **479** (4), 4665–4680 (2018), doi:10.1093/mnras/sty1529.

93. A. Sosa, J. A. Fernández, Cometary masses derived from non-gravitational forces. *Monthly Notices of the Royal Astronomical Society* **393** (1), 192–214 (2009), doi:10.1111/j.1365-2966.2008.14183.x.

94. T. D. Campbell, R. Febrian, J. T. McCarthy, H. E. Kleinschmidt, J. G. Forsythe, P. J. Bracher, Prebiotic condensation through wet–dry cycling regulated by deliquescence. *Nature Communications* **10** (1), 4508 (2019).

95. J. Korenaga, Hadean geodynamics and the nature of early continental crust. *Precambrian Research* **359**, 106178 (2021), doi:10.1016/j.precamres.2021.106178.

96. G. W. Wetherill, Collisions in the Asteroid Belt. *Journal of Geophysical Research* **72**, 2429 (1967), doi:10.1029/JZ072i009p02429.

97. H. Boehnhardt, R. P. Binzel, *Split Comets* (University of Arizona Press), pp. 301–316 (2004), `http://www.jstor.org/stable/j.ctv1v7zdq5.25`.

98. S. Müller, J. Baron, R. Helled, F. Bouchy, L. Parc, The mass-radius relation of exoplanets revisited. *Astronomy & Astrophysics* **686**, A296 (2024), doi:10.1051/0004-6361/202348690.

Acknowledgments

The authors thank M. Wyatt, T. Constantinou, and S. White for helpful discussions.

Funding: R.J.A. acknowledges the Science and Technology Facilities Council (STFC) for a PhD studentship. C.H.M. gratefully acknowledges the Leverhulme Centre for Life in the Universe at the University of Cambridge for support through Joint Collaborations Research Project Grant GAG/382. A.B. acknowledges the support of a Royal Society University Research Fellowship, URF/R1/211421.

Author contributions: Conceptualization, methodology, and visualization: R.J.A., C.H.M, and A.B. Formal analysis, and software: R.J.A. Manuscript drafting: R.J.A., C.H.M, A.B., P.B.R., and A.S.P.R. Project supervision: A.B., and P.B.R.

Competing interests: The authors declare that they have no competing interests.

Data and materials availability: No new data were generated for this work. Scripts used to generate the figures presented in this work will be made publicly available at `https://github.com/richard17a/comet_delivery_hcn`.

Supplementary materials

Materials and Methods

Supplementary Text

Figs. S1 to S8

Tables S1 to S2

References *(81-98)*

Supplementary Materials for

Cometary impacts an unlikely pathway towards the origins of life on Earth

Richard J. Anslow*, Catriona H. McDonald, Amy Bonsor, Paul B. Rimmer,

Auriol S. P. Rae

*Corresponding author. Email: rja92@cam.ac.uk

This PDF file includes:

Materials and Methods

The size-frequency distribution of Earth-crossing comets

The dynamical simulations of Nesvorný et al. (*27*) require some physical mechanism to limit the number of perihelion passages of small comets to match the observed modern-day population of ecliptic comets. Given that the physical lifetimes of modern JFCs are an order of magnitude shorted than their dynamical lifetimes, and that observations demonstrate the frequent disruption of comets (*33–35*), this is primarily attributed to cometary fragmentation (*27*).

While the precise cause(s) of cometary fragmentation remain debated, asymmetric outgassing has recently emerged as a leading mechanism through which cometary nuclei can be spun-up to their rotational disruption limits (*37–40*). Indirect evidence supporting the dominant role of rotational disruption is provided, on a population level, by modern JFCs, which exhibit a 'spin-barrier' in their radius-rotation period distribution, indicative of a population strongly sculpted by the effects of rotational instability (*37, 38, 41*). This is further supported by the observed break-up of Comet 332P/Ikeya–Murakami (*35*) and Comet 157P/Tritton (*40*), both consistent with rotational spin-up to the point of rotational instability. Finally, we note that the timescale of rotational spin-up is highly size-dependent [(*37*); see also Supplementary Text], satisfying the requirement for smaller comets to have shorter physical lifetimes (*27, 32*).

We follow a similar procedure to Rigley & Wyatt (*74*) in numerically determining the size-frequency distribution (SFD) of Earth-crossing comets subject to rotational instability. We consider comets in the size range $0.1 - 1000$ km, divided into 80 logarithmically spaced bins, with initial SFD as they're scattered into the inner Solar System represented by a broken power-law distribution, defined such that the number of comets of radius R is given by

$$n(R)dR = KR^{-\alpha}dR. \tag{S1}$$

The power law indices α are derived from available constraints from JFCs and the Kuiper belt (summarised in Table S1), while the constants of proportionality K in each size-range are constrained via the continuity of the size distribution.

Comets are added from the source region every 12000 yr – the physical lifetime of modern JFCs (*36*) – with the number of comets added to each size bin sampled randomly from a Poisson

distribution with mean value given by the input SFD (Table S1). The probability a comet fragments per time-step (δt) is given by

$$f(R) = \frac{\delta t}{\tau_{\rm ri}(R)}, \tag{S2}$$

where

$$\tau_{\rm ri}(R) = 100 \left(\frac{R}{1\ {\rm km}}\right)^2\ {\rm yr} \tag{S3}$$

is the (size-dependent) timescale of rotational instability [Jewitt (*37*); see Supplementary Text]. If fragmentation occurs, determined by sampling a random number in the range $[0, 1]$, it is assumed that two equal-mass child fragments are produced, distributed into the corresponding radius bin.

This population of comets, subject to losses via rotational instability, is integrated for 10 Myr (with a timestep $\delta t = 1$ yr) until the SFD reaches a steady-state; which we ensure is insensitive to the choice of timestep. The strong dependence of physical lifetime on comet radius is evident, with the slope of the SFD significantly shallower than the source population at small sizes. For $0.1 - 1$ km comets, the slope of the cumulative SFD decreases from -1.25 to -0.78, and for $1 - 50$ km comets, the slope decreases from -2.0 to -1.34. The SFD at larger sizes is relatively unaltered, with the slope decreasing from -5.0 to -4.78 for comets in the size range $50 - 150$ km.

We note that the resulting steady-state SFD is reassuringly insensitive to the assumed mechanism of comet fragmentation. Adopting instead the Di Sisto et al. (*32*) model of comet fragmentation – which is agnostic of physical break-up mechanism – we recover a SFD with slopes -0.78, -1.34 and -4.74 respectively. This is in surprising agreement with the Jewitt (*37*) model, and crucially, also implies a dramatic reduction in the number of small comets on Earth-crossing orbits.

Earth's cometary impact chronology

Given the inability of the lunar crater record to constrain both the bombardment history of the Earth-Moon system pre-3.92 Gya (*30*) and impactor composition (*29*), we instead leverage Earth's cometary bombardment chronology as derived from numerical N-body modelling of short-period comet formation and evolution (*26, 27*).

We anchor Earth's cometary bombardment to the flux of $D > 10$ km comets reported in Nesvorný et al. (*26*), given this subset of comets is least vulnerable to rotational instability. The

cumulative flux of $D > 10$ km comets is distributed in time according to

$$F(D > 10\,\mathrm{km}, t) = \frac{1}{6}\left[F_1 \exp\left\{-\left(\frac{t}{\tau_1}\right)^{\alpha_1}\right\} + F_2 \exp\left\{-\left(\frac{t}{\tau_2}\right)^{\alpha_2}\right\} + F_3\,(4570 - t)\right], \quad \text{(S4)}$$

where $F_1 = F_2 = 5.6 \times 10^3$, $\tau_1 = 7$ Myr, $\alpha_1 = 1$, $\tau_2 = 13$ Myr, $\alpha_2 = 0.44$, and $F_3 = 4 \times 10^{-3}$.

The impact flux of smaller comets is constrained by the steady-state SFD of Earth-crossing comets, and the continuity of the SFD at $D = 10$ km,

$$F(D, t) = F(D > 10\,\mathrm{km}, t)\left\{\frac{K(D)}{K(D > 10\,\mathrm{km})}\right\}, \quad \text{(S5)}$$

where

$$K(D) = D_{12}^{\alpha_1-\alpha_2}\int_{0.1}^{D_{12}} D^{-\alpha_1}dD + \int_{D_{12}}^{D_{23}} D^{-\alpha_2}dD + D_{23}^{\alpha_3-\alpha_2}\int_{D_{23}}^{D_{34}} D^{-\alpha_3}dD + D_{34}^{\alpha_4-\alpha_2}\int_{D_{34}}^{1000} D^{-\alpha_4}dD, \quad \text{(S6)}$$

and

$$K(D > 10\,\mathrm{km}) = \int_{10}^{D_{23}} D^{-\alpha_2}dD + D_{23}^{\alpha_3-\alpha_2}\int_{D_{23}}^{D_{34}} D^{-\alpha_3}dD + D_{34}^{\alpha_4-\alpha_2}\int_{D_{34}}^{1000} D^{-\alpha_4}dD. \quad \text{(S7)}$$

Here, we have defined the transition diameters $D_{12} = 1$ km, $D_{23} = 50$ km, $D_{34} = 150$ km, which relate to the power-law indices $\alpha_1 = 1.78$, $\alpha_2 = 2.34$, $\alpha_3 = 5.78$, $\alpha_4 = 3.5$ respectively.

The impact velocity distribution of short-period comets

To quantify the cometary delivery of prebiotic feedstock molecules, we must specify the velocity distribution of incident comets, given this largely controls the survival of fragile feedstock molecules during hypervelocity impact (*20, 22*).

Nesvorný et al. (*26*) record the mean impact velocities of comets, using an Öpik-like algorithm, onto the terrestrial planets, finding $[19.7, 28.2, 36.8]$ km s^{-1} onto Mars, Earth and Venus respectively. Motivated by the impact velocity distribution of meteoroids onto the modern Earth (*75, 76*), we sample impact velocities from a log-normal distribution,

$$dF(v_{\mathrm{imp}}; \mu, \sigma) = \frac{1}{\sigma v_{\mathrm{imp}}\sqrt{2\pi}} \exp\left(-\frac{(\ln v_{\mathrm{imp}} - \mu)^2}{2\sigma^2}\right) dv_{\mathrm{imp}}, \quad \text{(S8)}$$

where μ is the mean, and σ the standard deviation of the logarithm of the impact velocity v_{imp}.

Nesvorný et al. (*26*) do not record the standard deviation of comet impact velocities; motivated by the results of alternative dynamical simulations of Earth's cometary bombardment (*71*), and the modern velocity distribution of both short-period comets (*77*) and small meteoroids (*76*), we adopt a velocity dispersion of 5 $\mathrm{km\,s^{-1}}$.

The entry angle distribution of comets

Comets are assumed to arrive at the top of the atmosphere with a range of entry angles distributed according to the canonical Shoemaker (*78*) distribution,

$$dF(\theta) = \sin 2\theta d\theta. \tag{S9}$$

This distribution accounts for the gravitational focussing of comets by Earth, and corresponds to a most probable entry angle of 45°. Half of all cometary impacts will have entry angle in the range $30 - 60°$, while less than 7% of comets will arrive with entry angle shallower than 15° or steeper than 75°.

The effects of atmospheric entry on Earth's cometary impact flux

Given the low density and weak mechanical strength of cometary nuclei (*43*), even relatively large comets will be significantly decelerated during atmospheric passage, while small comets will catastrophically fragment at high altitudes (*25, 44, 79*). A direct consequence of atmospheric entry is that the distribution of comets reaching Earth's surface will differ significantly from the population incident at the top of the atmosphere.

We use the ATMOSENTRY code (*25*) to model the interaction of comets with the atmosphere, and record the size, velocity, and angle of comets directly before hypervelocity impact. This numerical model, described in detail in Anslow et al. (*25*), includes semi-analytical parametrisations for the ablation, deformation and fragmentation of comets during atmospheric entry. Key model parameters, consistent with previous literature [e.g., (*25, 44, 79*)] are described below.

Given scarce geological constraints on the Hadean atmosphere (*45*), we make the simplifying assumption of an isothermal atmosphere with density profile

$$\rho_{\mathrm{atm}}(z) = \rho_{\mathrm{surf}} \exp\left(-\frac{z}{H}\right), \tag{S10}$$

with scale height $H = 7.2$ km and surface density $\rho_{\rm surf} = 1.225\ {\rm kg\,m^{-3}}$, roughly consistent with Earth's modern atmosphere. We assume a cometary bulk density of $0.6\ {\rm g\,cm^{-3}}$ (*41*) and tensile strength 10^4 Pa (*43*). These are both upper limits, ensuring our results will present a best-case scenario for the cometary delivery of prebiotic feedstock molecules.

Exposed land on the early Earth

The dilution of prebiotic feedstock molecules during cometary impacts into global oceans presents a major concern, with only impacts onto subaerial land able to deliver a prebiotically plausible concentration of HCN. The extent of exposed land on the early Earth remains, however, highly uncertain (*49*). Moreover, while there exist many models of continental growth, these are crucially not direct proxies for exposed landmass given the non-monotonic history of ocean volume [(*49*); see Supplementary Text for further discussion].

For simplicity, given the significant uncertainty in estimates of exposed land on the early Earth, we adopt the McCulloch & Bennett (*50*) model of continental growth as a proxy for exposed landmass (following (*51*)). As noted in Bada & Korenaga (*52*), this is likely a large overestimate, which guarantees that our results represent an upper limit on the number of successful cometary impacts onto the early Earth. In this model, crustal surface area increases linearly from 0 to 12.8% of the modern value between $4.5 - 3.7$ Gya, such that the fraction of exposed land is given by

$$f_{\rm cc} = 0.0656t, \tag{S11}$$

where t is in Gyr.

While there remains significant debate regarding the growth of continental crust, there exists consensus with respect to the limited extent of continental crust during the early Hadean. Indeed, it is plausible that exposed land was limited to hotspot oceanic islands (*49, 52*). Given the rapid decline in Earth's cometary bombardment (*26*), the divergence of these models at later times has very little influence on our results; adopting instead a model that favours much quicker crustal formation (*80*), the number of successful impacts onto Earth increases by only a factor of 3 (Supplementary Text).

Monte Carlo simulation of Earth's cometary bombardment

To quantitatively investigate the successful cometary delivery of prebiotic feedstock molecules we employ Monte Carlo simulation, discretising Earth's cometary impact flux into 1 Myr timesteps. At each timestep, t_i, the expected number of cometary impacts onto exposed land, $\bar{N}_i$, is given by

$$\bar{N}_i = [F(D > 100\text{ m}, t_i) - F(D > 100\text{ m}, t_{i+1})]\, f_{\text{cc}}(t_i), \tag{S12}$$

where, recall, $F(D > 100\text{ m}, t_i)$ is the cumulative number of $D > 100$ m cometary impacts at t_i, and $f_{\text{cc}}(t_i)$ is the available exposed landmass. This is, generally, not an integer; the number of cometary impacts, N_i, at each timestep is thus sampled from a Poisson distribution with mean value $\bar{N}_i$. We note that $D < 100$ m comets will catastrophically airburst at high altitude (*25*), which allows us to limit the number of number of comets sampled, and thereby greatly decrease the computational cost of these simulations.

At each timestep we generate comets' radii, velocities, and entry angles at the top-of-atmosphere from the analytical distributions described previously. The effects of atmospheric entry are then calculated for each comet, determining the final distribution of radii, velocities, and angles at the surface. Not all comets will survive atmospheric entry, depending primarily on their initial size and entry angle; the number of comets reaching the surface will therefore be less than N_i.

For the subset of comets surviving atmospheric entry, we finally determine the fraction of HCN surviving hypervelocity impact. Comets are assumed to have an initial HCN concentration of 0.1 wt %, consistent with Solar System comets (*17*), and we use the parametrisation presented in McDonald et al. (*22*) (Eqs. 14-15), assuming equilibrium chemistry. To remain consistent with the parameter space investigated in (*22*), we discard any fragments of comets smaller than 100 m that reach the surface, and any comets with impact angle shallower than 15°.

This corresponds to an extremely small region of parameter space; less than 7% of comets arrive with entry angle less than 15°, with only much larger (roughly km-scale) comets able to survive atmospheric entry due to the increased atmospheric path (*25*). Moreover, atmospheric entry acts to increase impact angles towards the normal (see Fig. 2); this restriction therefore affects only km-scale comets with entry angles less than 15°. Finally, as discussed in (*25*), only a small subset of comets will generate $D < 100$ m fragments that reach Earth's surface; these fragments are expected to be highly thermally processed, and thus constitute an unlikely source of concentrated HCN.

To account for the inherent stochasticity when sampling from the respective distributions, we repeat this procedure 10^5 times, recording the number of successful cometary impacts as a function of time.

Supplementary Text

Jupiter-family comets' rotational spin-barrier

The vulnerability of cometary nuclei to rotational instability is evidenced by the so-called 'spin-barrier' – a critical rotation period below which large (gravity-dominated) comets fragment due to centripetal forces (*38, 41*). While previous studies have, in detail, calculated this critical period for both spheres (*81*) and triaxial ellipsoids (*82*), we motivate here this critical period following approximately the heuristic derivation presented in (*83*).

Consider a spherical nucleus comprising two hemispheres of radius R, with rotation period $P_{\rm rot}$. Each hemisphere's centre of mass will have radial velocity

$$v_r = \frac{3\pi R}{4P_{\rm rot}}, \tag{S13}$$

and will therefore experience an outwards centrifugal acceleration

$$a_c = \frac{3\pi^2 R}{2P_{\rm rot}^2}. \tag{S14}$$

When this acceleration exceeds both the comet's self-gravity and tensile strength, the comet will break-up; comets will therefore break-up with rotation periods smaller than

$$P_{\rm crit} = R\left(\frac{\rho\pi^2}{\sigma_T(1+\kappa)}\right)^{1/2} \tag{S15}$$

where $\kappa = (64/81)\cdot\pi G\rho^2 R^2/\sigma_T$, ρ is the comet's bulk density and σ_T its tensile strength. This is in agreement with the more detailed calculation in (*81*) to order unity.

It is clear from Equation S15 that this critical rotation period has very different behaviour in the large and small radius limits. For large comets, self-gravity dominates such that $P_{\rm crit}$ is independent of both size and tensile strength,

$$P_{\rm crit}^{\rm grav} \simeq \left(\frac{3\pi}{\rho G}\right)^{1/2} \simeq 4.26\ \left(\frac{\rho}{0.6\ {\rm g\,cm^{-3}}}\right)^{-1/2}\ {\rm hr}. \tag{S16}$$

In contrast, small comets are strength-dominated with a critical rotation period dependent on both radius and tensile strength,

$$P_{\rm crit}^{\rm str} \simeq \left(\frac{\rho\pi^2}{\sigma_T}\right)^{1/2} R. \tag{S17}$$

This critical rotation period is compared against modern JFCs (*41*) and small asteroids (*84*) in Fig. S1. All comets in this sample are stable against rotational instability when assuming tensile strengths of the order $1 - 10$ Pa. This is consistent with the typical tensile strength of cometary nuclei, which lie in the range $\sim 1 - 100$ Pa (*43, 85*).

We further note that the median rotation periods of comets is significantly larger than that of asteroids (*37, 86*), consistent with the much weaker tensile strength of cometary nuclei. The simplest explanation for these data is that the observed rotation period distributions reflect the density dependence of $P_{\rm crit}$, and that the current-day JFC population is strongly sculpted by the effects of rotational instability (*37*).

The timescale of rotational spin-up

It is well established observationally, in the form of significant non-gravitational accelerations, that the orbits of comets are perturbed by reactive forces in response to outgassing (*87, 88*). A net torque is a natural by-product of non-uniform mass loss (e.g., due to an asymmetric spatial distribution of vents (*37, 89*)), which will change the direction and magnitude of a comet's spin angular momentum. Given that it is difficult observationally to determine a comet's spin axis, rotation period is typically used as a radily accessible proxy for this evolution (*89–91*).

Rotational spin-up is investigated in detail in Jewitt (*37*), using a sample of published rotation periods and period changes for JFC nuclei (*92*). Here, we motivate the size-dependence of the timescale for outgassing to spin-up cometary nuclei to the point of rotational instability, following simple (largely dimensional) arguments.

We consider a spherical nucleus, radius R, experiencing a reactive force $\boldsymbol{F}_{\rm ng}$ due to anisotropic outgassing. Its change in angular velocity $\Omega = |\boldsymbol{\Omega}|$ will be given by

$$I\dot{\Omega} = \tau_\Omega, \tag{S18}$$

where I is the comet's moment of inertia and $\tau_\Omega = \boldsymbol{\tau} \cdot \boldsymbol{\Omega}/\Omega$ is the component of the net torque $\boldsymbol{\tau}$ along $\boldsymbol{\Omega}$.

Intuitively, the net torque should be related to the magnitude of the reactive force and size of the comet ($\boldsymbol{\tau} \sim \boldsymbol{R} \times \boldsymbol{F}_{\rm ng}$) via some effective (dimensionless) moment arm, ξ [e.g., (*37, 90, 91*)], accounting for the fact that not all outgassed material will torque the comet. In the extreme cases, $\xi = 1$ corresponds to perfectly anisotropic (i.e., collimated) outgassing from the surface of the comet, while $\xi = 0$ corresponds to perfectly isotropic outgassing (generating no torque on the comet). The component of the net torque along $\boldsymbol{\Omega}$ is thus,

$$\tau_\Omega = \xi R F_{\rm ng}. \tag{S19}$$

Assuming spherical symmetry ($I = 2MR^2/5$), the comet's angular velocity will therefore evolve as

$$\dot{\Omega} = \frac{5\xi F_{\rm ng}}{2MR}, \tag{S20}$$

where M is the comet's mass.

It is natural to expect [and supported by observation of both short-and long-period comets (*37, 39*)] in the sublimative hypothesis of outgassing, that activity (and hence the magnitude of the net force acting on the comet) will be proportional to nucleus surface area and depend on distance from the Sun as r^{-2}, such that

$$F_{\rm ng} = \alpha_{\rm ng} M_0 \left(\frac{R}{R_0}\right)^{-2} \left(\frac{r}{r_0}\right)^{-2}, \tag{S21}$$

where $\alpha_{\rm ng}$ is the typical measured non-gravitational acceleration of short-period comets, R_0 (M_0) a characteristic comet radius (mass), and $r_0 \simeq 2.8$ au the characteristic orbital radius (*88*).

We therefore find

$$\dot{\Omega} = \frac{5\xi\alpha_{\rm ng}}{2R_0} \left(\frac{R}{R_0}\right)^{-2} \left(\frac{r}{r_0}\right)^{-2}. \tag{S22}$$

Small comets are particularly susceptible to torques driven by anisotropic outgassing, and will be rapidly spun-up to the point of rotational disruption.

We can finally calculate the number of orbits (N) required to spin-up a comet to the point of rotational instability by considering

$$\int_{\Omega_{\rm init}}^{\Omega_{\rm crit}} d\Omega = \frac{5\xi\alpha_{\rm ng} r_0^2}{2R_0} \left(\frac{R}{R_0}\right)^2 \int_0^{2\pi N} r^{-2} \frac{r^2 df}{na^2\sqrt{1-e^2}}, \tag{S23}$$

where (n, a, e, f) are the characteristic mean motion, semi-major axis, eccentricity and true anomaly of short-period comets. The corresponding timescale of rotational instability is therefore

$$\tau_{\rm ri} = \frac{2\pi N}{n} = \frac{4}{5} \left(\frac{aR_0\sqrt{1-e^2}}{\xi\alpha_{\rm ng} r_0^2}\right) (\Omega_{\rm crit} - \Omega_{\rm init}) \left(\frac{R}{R_0}\right)^2. \tag{S24}$$

To estimate this timescale for (Earth-crossing) short-period comets ($a \sim 4$ au, $e \sim 0.75$, $q \sim 1$ au), assuming an effective lever-arm $\xi \sim 0.006$ (*37, 91*), and a typical non-gravitational acceleration $\alpha_{\rm ng} \sim 10^{-9}$ au d^{-2} (*91, 93*), we find

$$\tau_{\rm ri} \sim 100 \left(\frac{R}{1 \text{ km}} \right)^2 \text{ yr}, \tag{S25}$$

recovering (to order of magnitude) the timescale found by Jewitt (*37*) – consistent with the observed spin-up of short-period comets with perihelia in the range $\sim 1 - 2$ au.

Sensitivity to exposed land on the early Earth

An important pre-requisite for the delivery of a prebiotically relevant concentration of HCN is impact onto exposed, subaerial land. Moreover, we note that many prebiotic chemical networks rely on short-term wet-dry cycling to drive the biogeochemical reactions required for the synthesis of key biopolymers (*51, 94*). However, despite its central importance for many origins of life scenarios, the extent of exposed land on the early Earth remains poorly constrained (*49*). Further, while there exist many models of continental growth on the early Earth [see (*95*) and references therein], these are not direct proxies for exposed landmass, given the non-monotonic history of ocean volume (*49*).

In the interest of simplicity, we therefore adopt the McCulloch & Bennett (*50*) model of continental growth as a proxy for exposed landmass (following (*51*)). While this is likely a large overestimate of exposed landmass, given the potential for global oceans to limit subaerial landmass to hotspot oceanic islands (*52*), this guarantees that our results represent a best-case scenario for the cometary delivery of prebiotic feedstock molecules.

If we were instead to adopt the Guo & Korenaga (*80*) model of continental growth, which favours much quicker crustal formation compared to the rather than McCulloch & Bennett (*50*) model (Fig. S2), the number of impacts delivering > 10 mM HCN increases by only a factor of 3 (Table S2). This indicates that our results are insensitive to the significant uncertainty in models of continental growth, which is a consequence of the rapid decline in Earth's cometary impact flux (*26*), and the relative consensus between models regarding the very limited extent of exposed land during the early Hadean.

Sensitivity to dynamical model of Earth's cometary bombardment

Monte Carlo simulations using the Brasser et al., (71) impact chronology. Despite our Monte Carlo simulations, when adopting the Nesvorný et al. (*26*) chronology, recording total cometary mass accretion of $(2.63 \pm 0.10) \times 10^{18}$ kg – consistent with independent constraints on Earth's cometary accretion (*46, 47*) – we could equally have adopted an alternative model of Earth's cometary bombardment. This choice will, in principle, change the velocity distribution and timing of cometary impacts onto Earth, and therefore has the potential to affect the number of successful cometary impacts.

Here, we test our sensitivity to the assumed dynamical model of cometary bombardment, adopting instead the Brasser et al. (*71*) impact chronology. This study determines the initial conditions most likely to reproduce the modern-day architecture of the Solar System's giant planets, and given these initial conditions calculates the fraction of comets in the trans-Neptunian disk that enter the inner Solar System. The temporal mass of comets crossing 1.7 au is parametrised as

$$M_c = 4M_E \sum_{i=1}^{3} a_i \exp\left(\frac{4500 - t}{\tau_i}\right), \tag{S26}$$

where a_i and τ_i are fitting constants, and M_E is the mass of the Earth. Cometary mass accretion to the early Earth is encapsulated via a mean impact probability, $p_{\rm imp} = 3.1 \times 10^{-8}$. This corresponds to a total mass accretion of 1.1×10^{19} kg, again roughly consistent with available isotopic constraints (*46, 47*).

At each timestep, t_i, in our Monte Carlo simulation, total cometary mass accretion to the Earth is therefore

$$\delta m_i = [M_c(t_i) - M_c(t_{i+1})]\, p_{\rm imp}. \tag{S27}$$

Given the steady-state SFD of Earth-crossing comets, this determines the constants of proportionality K_i at each timestep via

$$\delta m_i = \frac{\pi\rho}{6}\left\{K_1 \int_{0.1}^{1} D^{3-\alpha_1} dD + K_2 \int_{1}^{50} D^{3-\alpha_2} dD + K_3 \int_{50}^{150} D^{3-\alpha_3} dD + K_4 \int_{150}^{1000} D^{3-\alpha_4} dD\right\}, \tag{S28}$$

and the continuity of the SFD. The mean number of cometary impacts, $\bar{N}_i$ is then

$$\bar{N}_i = K_1 \int_{0.1}^{1} D^{-\alpha_1} dD + K_2 \int_{1}^{50} D^{-\alpha_2} dD + K_3 \int_{50}^{150} D^{-\alpha_3} dD + K_4 \int_{150}^{1000} D^{-\alpha_4} dD. \tag{S29}$$

As before, this will not typically be an integer, and we therefore determine the number of cometary impacts, N_i, by sampling from a Poisson distribution with mean value $\bar{N}_i$.

The Brasser et al. (*71*) simulations record a much lower mean impact velocity of only $\langle v_{\rm imp} \rangle = 22\ {\rm km\,s^{-1}}$, which we use in our Monte Carlo simulations. A by-product of the much lower mean velocity is an increase in the collisional impact probability (*96*); relative to the Nesvorný et al. (*26*) chronology, there is a rapid decrease in Earth's cometary impact flux. The results of this comparison are shown in Fig. S3, which clearly demonstrates the more rapid decline impact flux in the Brasser et al. (*71*) chronology.

Despite the greater overall cometary mass accretion, and lower mean impact velocity, the median number of cometary impact delivering > 10 mM HCN is still only 1 – exactly the same as with the Nesvorný et al. (*26*) chronology. The distribution in total number of successful impacts is shown in Fig. S4, highlighting that the number of simulations recording no successful cometary impacts is in fact substantially greater with the Brasser et al. (*71*) chronology. This is a consequence of the rapid decline in impact flux, which exacerbates the tension with the slow growth of exposed landmass during the early Hadean (*49*). The results of this comparison are thus reassuring, with two independent dynamical models of Earth's cometary bombardment in agreement that there was, in this best-case scenario, one successful impact at very early times.

Sensitivity to assumed mechanism of comet fragmentation

Motivated by the results of dynamical simulations of short-period comet formation (*27, 32*), and the short physical lifetime of JFCs (*36*), we numerically modelled the effects of cometary fragmentation on the SFD of Earth-crossing comets. While recent work indicates that rotational instability is a leading mechanism responsible for the the disruption of short-period comets (*37*), it is likely that other mechanisms contribute to the disruption of short-period comets [see (*97*) for a review of comet fragmentation].

Previous work (*74*) has remained agnostic to the responsible physical mechanism, adopting instead the Di Sisto et al. (*32*) prescription of comet fragmentation. This model assumes a constant probability of fragmentation per perihelion passage, and instead takes into account the fact that it will be harder for fragments to gravitationally escape from large comets (given that escape velocity $v_{\rm esc} = \sqrt{2GM/R} \propto R$ is proportional to radius). Small comets, with minimal self-gravity,

are unlikely to retain significant mass following fragmentation. The slope of the steady-state SFD remains essentially unchanged if we were to instead use the Di Sisto et al. (*32*) model of comet fragmentation. The results of our Monte Carlo calculation remain unchanged when using the Di Sisto et al. (*32*) model of cometary fragmentation; only 1 cometary impact delivers > 10 mM HCN.

Which comets deliver prebiotically relevant concentrations of HCN?

To highlight the subset of comets incident at the top of Earth's (and indeed also Mars and Venus) atmosphere responsible for the delivery of a prebiotically relevant concentration of HCN, we compare in Figs. S5–S7 the distribution of comets at the top-of-atmosphere with the population that subsequently deliver > 10 mM HCN.

For Earth and Mars, it is evident that the impact velocity distribution of comets incident on each planet largely controls the survival of HCN during hypervelocity impact. To moderate the peak temperatures – and associated destruction of HCN – highly-oblique impacts are required. This is seen clearly in Figs. S5 and S6 for which there are tight correlations between impact velocity and angle for those comets delivering a prebiotically relevant concentration of HCN. The dominant role played by entry angle is evidenced by the distribution of entry angles of successful cometary impacts, which bears little resemblance to the overall distribution of comets arriving at the top-of-atmosphere.

The picture is more complicated for Venus, which has significantly less cometary impacts delivering a prebiotically relevant concentration of HCN relative to both Mars and Earth. The key differences are driven by Venus' dense atmosphere, which drives the destruction of very large km-scale comets. Perhaps counter-intuitively, the velocity distribution of comets appears to make little effect on the survival of HCN. It is instead the size of comets controlling the delivery of high concentrations of HCN; comets with initial radius $\sim$ 3 km, aero-braked to very low velocities, that dominate the delivery of prebiotically relevant concentrations of HCN. This corresponds to a vanishingly small corner of parameter space, sampling the largest sizes in the comets' SFD, and it remains a possibility that there is additionally the significant destruction of HCN during the fragmentation of these comets near to Venus' surface (*25*).

Exoplanet escape velocities

To demonstrate the radius-dependence of planetary escape velocity, we use data from the PlanetS catalogue (`https://dace.unige.ch/`), which comprises 860 exoplanets with well-characterised masses and radii (i.e., relative measurement uncertainties less than 25% and 8% respectively). The distribution of this catalogue of exoplanets in mass-radius space is shown in Fig. S8, with the (piece-wise) data-driven mass-radius relationship from Müller et al. (*98*) included for reference. For Earth-like exoplanets (i.e., masses less than roughly $4M_E$), the escape velocity scales as

$$v_{\rm esc} = \sqrt{\frac{2GM_{\rm pl}}{R_{\rm pl}}} \propto M_{\rm pl}^{0.365} \tag{S30}$$

an increasing function of exoplanet mass. Escape velocity as a function of planet radius is shown in the lower panel of Fig. S8; only 5 exoplanets in the PlanetS catalogue (0.58%) have escape velocity less than Earth's. These are all above Mars' escape velocity, with the lowest escape velocity in the sample 7.4 $\mathrm{km\,s^{-1}}$.

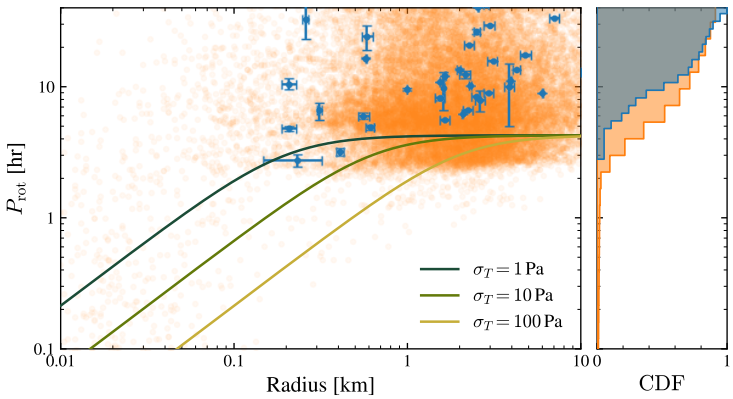

Figure S1: **Modern Jupiter-family comets' radius-rotation period distribution is strongly sculpted by rotational instability.** Cometary rotation periods and radii are taken from (*41*) (blue), while the rotation periods and radii of small asteroids are from (*84*) (orange); the cumulative distribution function (CDF) of rotation periods is shown in the right-hand panel. The minimum rotation periods stable to rotational instability are included for three representative tensile strengths in the range 1 – 100 Pa; all comets in this sample are stable to rotational instability. The small asteroids distribution shows significant differences to JFCs, consistent with a significantly increased tensile strength of small asteroids.

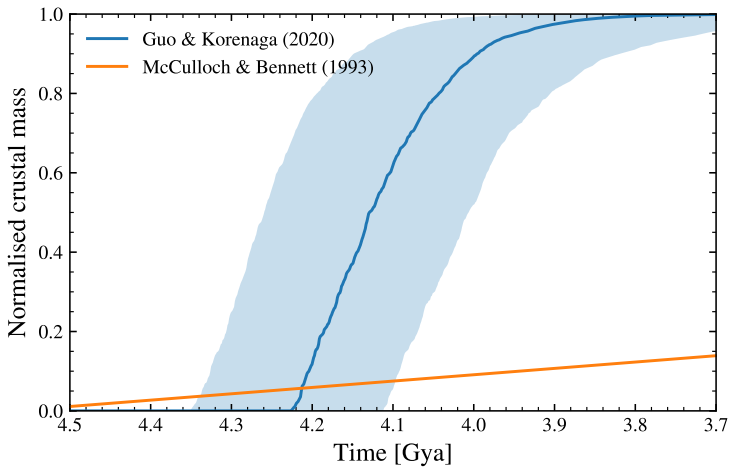

Figure S2: **Models of continental growth on the Hadean Earth.** Shown here are the McCulloch & Bennett (*50*) (orange) and Guo & Korenaga (*80*) (blue) models of continental growth, normalised to modern day continental crustal mass. These models are near end-member cases, describing respectively the slow and rapid growth of continental crust – an upper limit for subaerial land on the Hadean Earth. Only the central 50% of the Guo & Korenaga solutions are plotted for clarity.

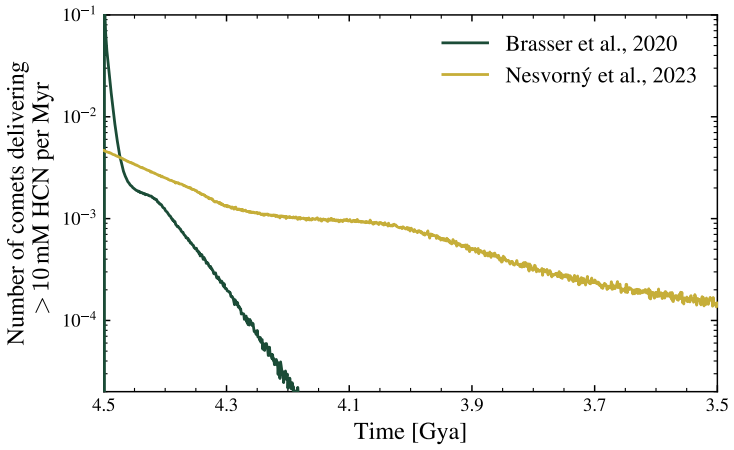

Figure S3: **Results from Monte Carlo simulation of Earth's early cometary bombardment demonstrate little sensitivity to the assumed model of cometary bombardment.** We vary only the dynamical model of Earth's cometary bombardment – using the Brasser et al. (*71*) chronology (blue) and Nesvorný et al. (*26*) chronology – and the comets' impact velocity distribution, keeping the assumed model of continental growth (*50*) constant. The median number of successful cometary impacts per Monte Carlo realisation is 1 in both cases, highlighting the insensitivity of our results to the assumed model of cometary bombardment.

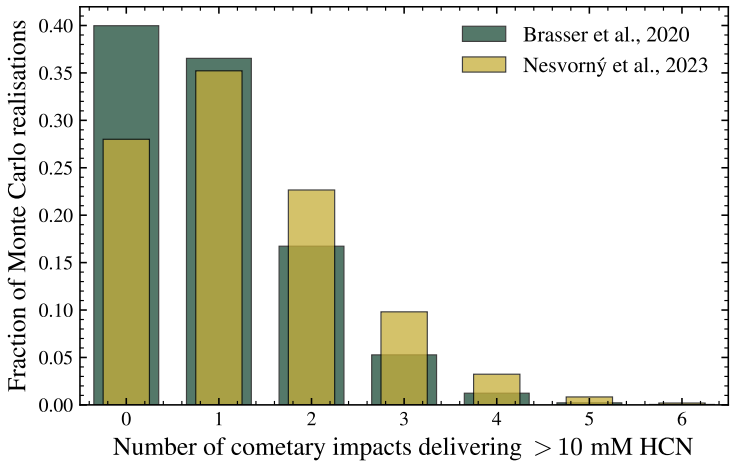

Figure S4: **The distribution of successful cometary impacts per Monte Carlo simulation.** The number of cometary impacts delivering > 10 mM HCN per Monte Carlo realisation of Earth's cometary bombardment history. The median number of successful impacts is one, with 28% of simulations recording no successful cometary impacts.

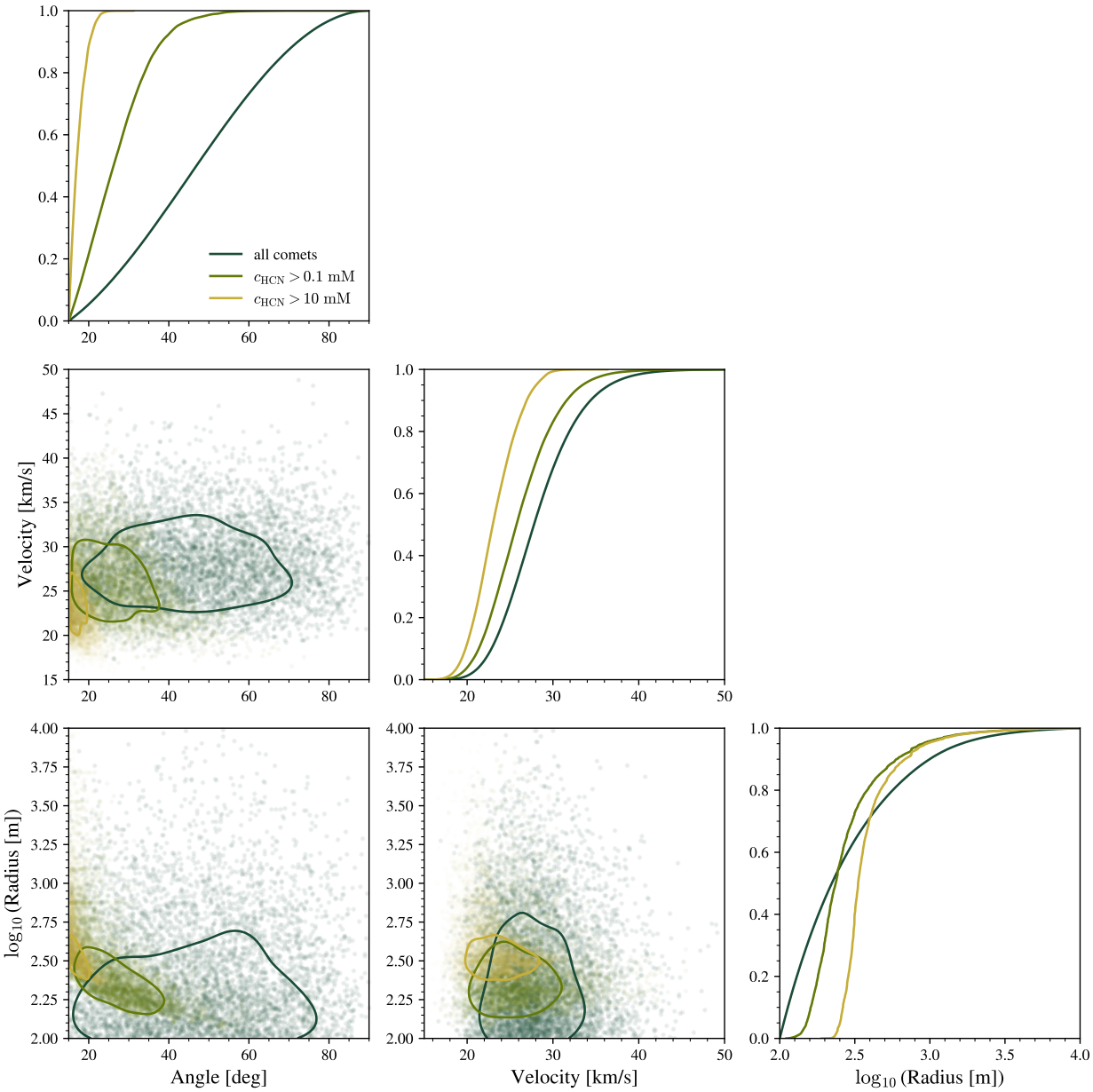

Figure S5: **The subset of comets delivering prebiotically relevant concentrations of HCN to the Earth.** The distribution of comets' impact velocities, sizes and entry angles at the top of the atmosphere (blue) is compared with the subset of these comets delivering 0.1 mM (green) and a prebiotically relevant concentration of HCN, 10 mM (yellow). The relationships between impact velocity, entry angle and initial radius are shown in the respective scatter plots.

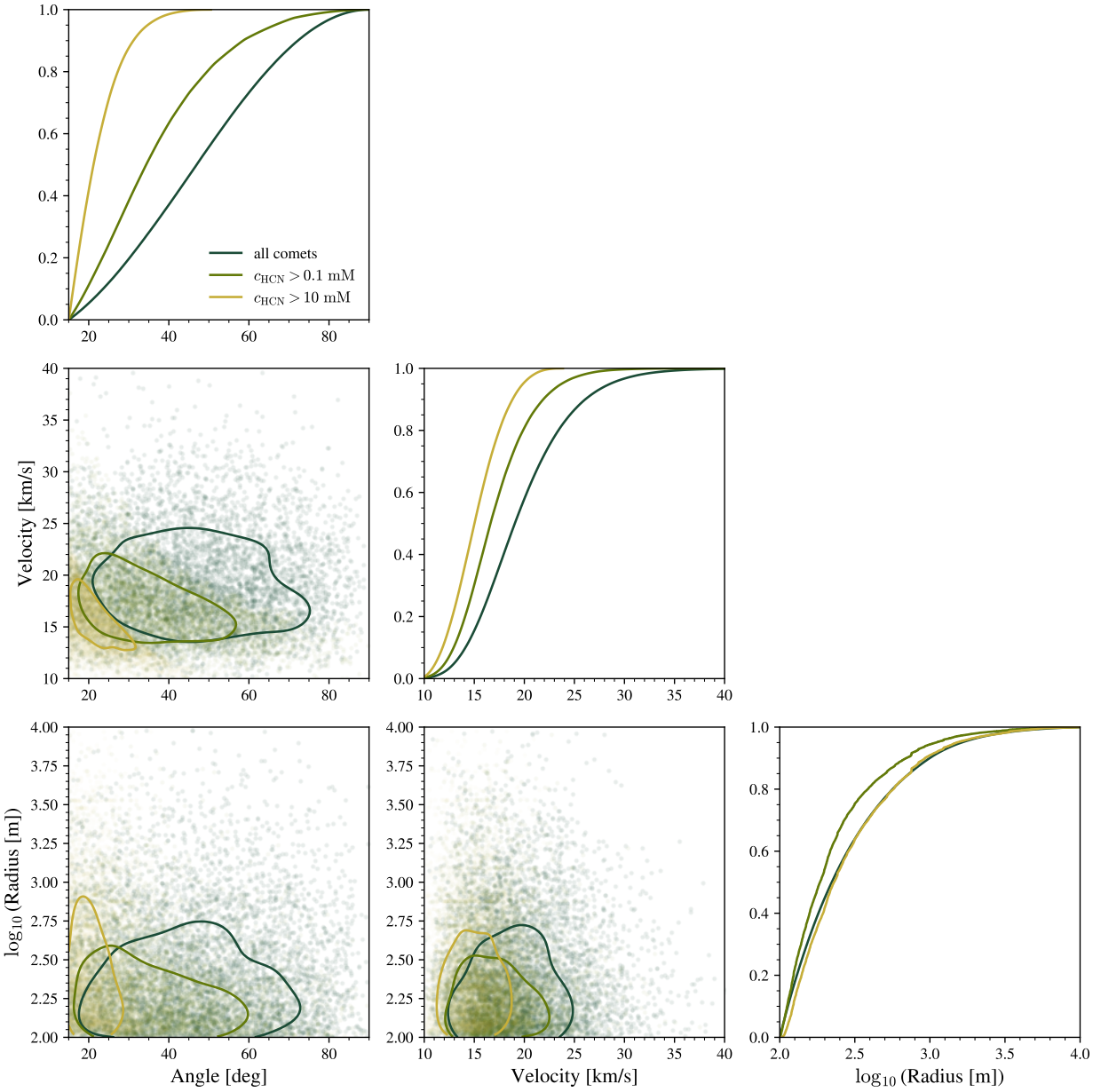

Figure S6: **The subset of comets delivering prebiotically relevant concentrations of HCN to Mars.** Same as Fig. S5, only for Mars – using Mars' cometary impact chronology, impact velocity distribution, and Mars' present-day 6 m bar atmospheric surface pressure.

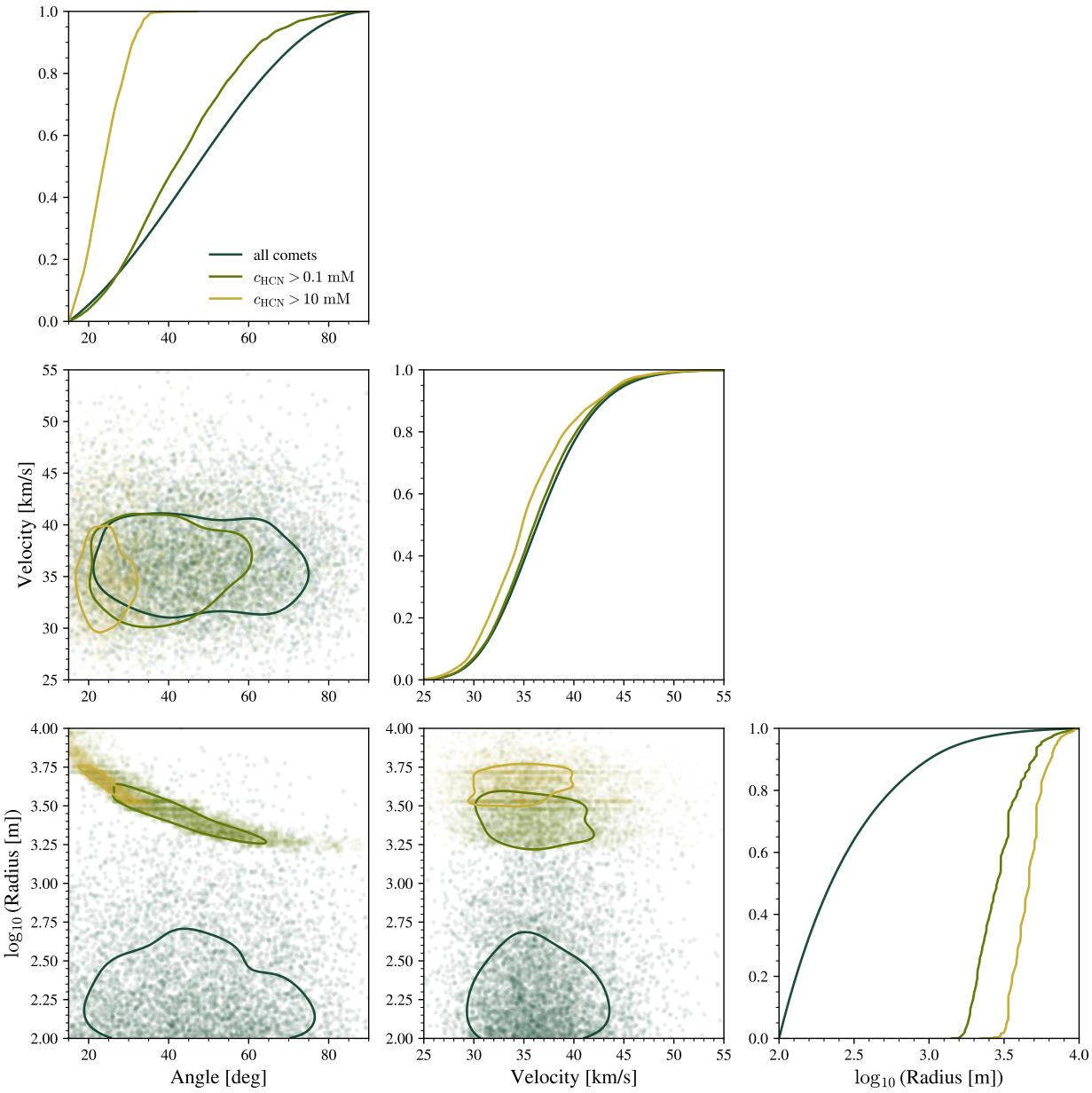

Figure S7: **The subset of comets delivering prebiotically relevant concentrations of HCN to Venus.** Same as Fig. S5, only for Venus – using Venus' cometary impact chronology, ipmact velocity distribution, and Venus' present-day 93 bar atmospheric surface pressure.

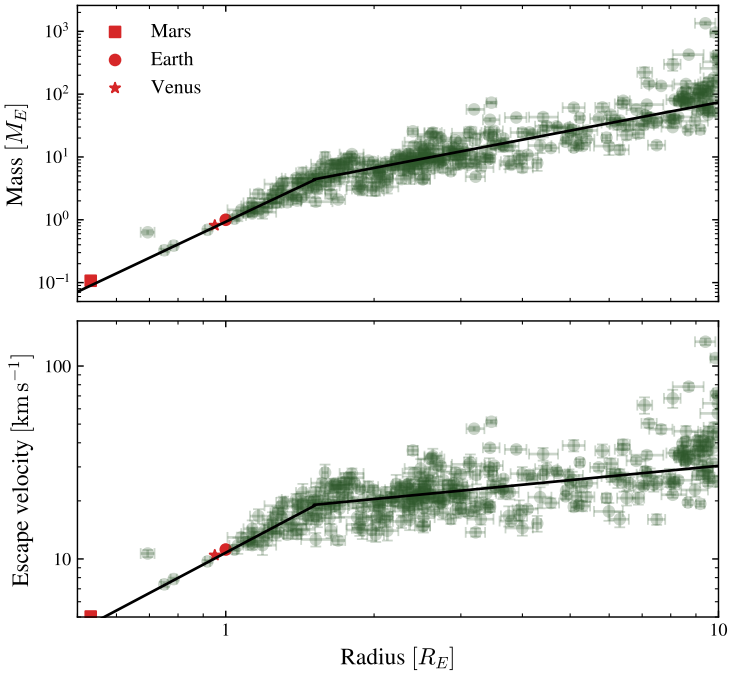

Figure S8: **The mass-radius distribution (top) and escape-velocity-radius distribution (bottom) of the PlanetS exoplanet catalogue.** Data from the PlanetS catalogue are displayed in green, with the Solar System's terrestrial planets included in red, and empirical mass-radius/escape velocity-radius relationships (*98*) included in black.

Size range [km]	α
$0.1 \leq R \leq 1$	2.25
$1 \leq R \leq 50$	3.0
$50 \leq R \leq 150$	6.0
$150 \leq R \leq 1000$	3.5

Table S1: **Slopes of the differential size-frequency distribution (SFD) of Jupiter-family nuclei.** This observationally motivated distribution is used in our numerical model as the SFD of comets input into the inner Solar System. The slope of the cumulative size distribution, often quoted in the literature is $\gamma = \alpha - 1$.

c_{HCN} [mM]	McCulloch & Bennett (1993)	Guo & Korenaga (2020)
0.1	41	87
1.0	13	32
10	1	3
30	0	0

Table S2: **The median number of impacts delivering HCN above a threshold concentration c_{HCN} to Earth when varying the assumed model of continental growth**. We use the near end-member cases of the McCulloch & Bennet (*50*) and (*80*) models as proxies for the slow and rapid growth of continental crust respectively.